Spindle checkpoint–independent inhibition of mitotic chromosome segregation by *Drosophila* Mps1

Friederike Althoff[a], Roger E. Karess[b], and Christian F. Lehner[a]
[a]Institute of Molecular Life Sciences, University of Zurich, 8057 Zurich, Switzerland; [b]Centre National de la Recherche Scientifique, Institut Jacques Monod, Unité Mixte de Recherche 7592, Université Paris Diderot, Paris Cedex 13, France

ABSTRACT **Monopolar spindle 1 (Mps1) is essential for the spindle assembly checkpoint (SAC), which prevents anaphase onset in the presence of misaligned chromosomes. Moreover, Mps1 kinase contributes in a SAC-independent manner to the correction of erroneous initial attachments of chromosomes to the spindle. Our characterization of the *Drosophila* homologue reveals yet another SAC-independent role. As in yeast, modest overexpression of *Drosophila Mps1* is sufficient to delay progression through mitosis during metaphase, even though chromosome congression and metaphase alignment do not appear to be affected. This delay in metaphase depends on the SAC component Mad2. Although *Mps1* overexpression in *mad2* mutants no longer causes a metaphase delay, it perturbs anaphase. Sister kinetochores barely move apart toward spindle poles. However, kinetochore movements can be restored experimentally by separase-independent resolution of sister chromatid cohesion. We propose therefore that Mps1 inhibits sister chromatid separation in a SAC-independent manner. Moreover, we report unexpected results concerning the requirement of Mps1 dimerization and kinase activity for its kinetochore localization in *Drosophila*. These findings further expand Mps1's significance for faithful mitotic chromosome segregation and emphasize the importance of its careful regulation.**

Monitoring Editor
Monica Bettencourt-Dias
Instituto Gulbenkian de Ciência

Received: Feb 14, 2012
Revised: Apr 17, 2012
Accepted: Apr 24, 2012

INTRODUCTION

Monopolar spindle 1 (Mps1) is required for the spindle assembly checkpoint (SAC), which inhibits exit from mitosis in the presence of misaligned chromosomes (Musacchio and Salmon, 2007). Moreover, Mps1 also contributes in a SAC-independent manner to the correction of initial erroneous chromosome attachments to the spindle during prometaphase (Jones *et al.*, 2005; Maure *et al.*, 2007; Jelluma *et al.*, 2008b; Hewitt *et al.*, 2010; Santaguida *et al.*, 2010; Sliedrecht *et al.*, 2010).

The mechanistic details of how Mps1 functions in mitotic regulation are complex and still poorly understood. The intracellular localization of Mps1 is highly dynamic (Fisk and Winey, 2001; Stucke *et al.*, 2002; Liu *et al.*, 2003; Fischer *et al.*, 2004; Howell *et al.*, 2004; Jelluma *et al.*, 2010; Zhang *et al.*, 2011). During interphase Mps1 resides primarily in the cytosol, with some enrichment on centrosomes and on the nuclear envelope becoming apparent in late G2. During prometaphase, a fraction of Mps1 accumulates rapidly and strongly on unattached kinetochores, with a residence time of only a few seconds (Howell *et al.*, 2004; Jelluma *et al.*, 2010). Attachment to the spindle correlates with disappearance of Mps1 from the kinetochore.

The high local concentration of Mps1 on unattached kinetochores makes a crucial contribution to SAC activation. It is likely to stimulate Mps1 kinase activity via Mps1–Mps1 protein interactions (Hewitt *et al.*, 2010) and autophosphorylation (Kang *et al.*, 2007; Mattison *et al.*, 2007; Jelluma *et al.*, 2008a; Dou *et al.*, 2011). Apart from Mps1 itself, some additional proteins involved in kinetochore attachment and SAC function (like borealin, BubR1, Cenp-E, Dam1, Mad1, Mad2, and Ndc80) have been shown to be Mps1 kinase substrates (Hardwick *et al.*, 1996; Shimogawa *et al.*, 2006; Espeut *et al.*, 2008; Huang *et al.*, 2008; Jelluma *et al.*, 2008b;

This article was published online ahead of print in MBoC in Press (http://www.molbiolcell.org/cgi/doi/10.1091/mbc.E12-02-0117) on May 2, 2012.
Address correspondence to: Christian F. Lehner (christian.lehner@imls.uzh.ch).
Abbreviations used: EGFP, enhanced green fluorescent protein; Mps1, monopolar spindle 1; SAC, spindle assembly checkpoint; TEV, tobacco etch virus.

Kemmler *et al.*, 2009; Zich *et al.*, 2012). Mps1 kinase activity is also known to regulate accumulation of the SAC components Mad1 and Mad2 at unattached kinetochores (Abrieu *et al.*, 2001; Martin-Lluesma *et al.*, 2002; Liu *et al.*, 2003; Tighe *et al.*, 2008; Hewitt *et al.*, 2010; Kwiatkowski *et al.*, 2010; Maciejowski *et al.*, 2010; Santaguida *et al.*, 2010; Sliedrecht *et al.*, 2010). Moreover, Mps1 activity at the kinetochore has been proposed to stimulate Mad1-dependent conformational change of Mad2 from an open to a closed form (Hewitt *et al.*, 2010; Maldonado and Kapoor, 2011) that is crucial for inhibition of the Cdc20-anaphase–promoting complex/cyclosome (Cdc20-APC/C; Luo *et al.*, 2002; Sironi *et al.*, 2002; DeAntoni *et al.*, 2005; Mapelli *et al.*, 2007; Fava *et al.*, 2011), the ubiquitin ligase that controls anaphase onset.

Besides accumulation at unattached kinetochores, subsequent removal of Mps1 after correct spindle attachment appears to be important. Expression of Mps1 variants fused to protein domains enforcing persistent localization to kinetochores even after correct bipolar attachment to the spindle was shown to prevent timely SAC silencing and anaphase onset in both human cells and fission yeast (Jelluma *et al.*, 2010; Ito *et al.*, 2012). Finally, Mps1 has also been proposed to act in the cytosol, where it promotes the formation of Cdc20-inhibitory complexes, including the SAC component BubR1 (Maciejowski *et al.*, 2010).

The molecular mechanisms controlling Mps1 kinetochore recruitment remain unclear. For example, some studies argued that Mps1's kinase activity is required for recruitment (Xu *et al.*, 2009; Colombo *et al.*, 2010), whereas others found that kinase activity stimulates its release from the kinetochore (Hewitt *et al.*, 2010; Jelluma *et al.*, 2010). The N-terminal region of human Mps1 is required for kinetochore localization, and the kinetochore protein Ndc80/Hec1 is clearly required for Mps1 accumulation at kinetochores (Martin-Lluesma *et al.*, 2002; Saurin *et al.*, 2011). In budding yeast, Mps1 binds directly to Ndc80 (Kemmler *et al.*, 2009), but the corresponding interaction has not been observed in animal cells. Aurora B might stimulate the Ndc80–Mps1 interaction, as this kinase is required for recruitment of normal levels of Mps1 to kinetochores and its activity phosphorylates Ndc80 (Cheeseman *et al.*, 2006; DeLuca *et al.*, 2006; Ciferri *et al.*, 2008), presumably in particular at unattached kinetochores that do not experience physical tension (Liu *et al.*, 2009; Welburn *et al.*, 2010). Mps1 disappearance after bipolar attachment of chromosomes to the spindle might therefore reflect reduced Ndc80 phosphorylation by Aurora B. Mps1 disappearance after kinetochore attachment presumably depends on additional pathways. After attachment, Mps1 is transported along kinetochore microtubules away from kinetochores like other SAC components (Pandey *et al.*, 2007). This shedding of SAC components from the kinetochore is known to be dynein dependent (Howell *et al.*, 2001; Wojcik *et al.*, 2001). Moreover, in budding yeast, APC/C-dependent proteolytic degradation of Mps1 during exit from mitosis prevents SAC reactivation (Palframan *et al.*, 2006). Similarly, Mps1 degradation during exit from mitosis has also been implicated in mammalian cells (Cui *et al.*, 2010).

Here we characterize Mps1 function in *Drosophila melanogaster*. As revealed by our initial analyses (Fischer *et al.*, 2004), *Drosophila Mps1* is essential for SAC function. In addition, it appears to have SAC-independent functions, since the phenotype caused by *Mps1*-null mutations is more severe than that of *mad2*-null and *bubR1*^{KEN} mutants. These last-named mutants clearly revealed that the SAC is not required for development into fertile adults in *Drosophila* (Buffin *et al.*, 2007; Rahmani *et al.*, 2009). Far fewer *Mps1*-null mutants develop into adults. Adult *Mps1* mutant females missegregate chromosomes during meiosis (Gilliland *et al.*, 2005, 2007). In fact, the first *Mps1* allele to be isolated is *altered disjunction*^{1} (*ald*^{1}), which results in chromosome missegregation during meiosis I (O'Tousa, 1982). Here we focus on mitotic functions. Using transgenic strains allowing expression of wild-type and mutant Mps1 versions in different genetic backgrounds, we analyze functional domains and reveal a novel SAC-independent role in the control of sister chromatid separation.

RESULTS

Kinase activity of *Drosophila* Mps1 is dispensable for self-association but required for kinetochore localization

In vivo imaging of a fully functional enhanced green fluorescent protein (EGFP)–Mps1 protein during the syncytial mitoses of early embryogenesis indicated that *Drosophila* Mps1 is localized to the kinetochore but only during the early mitotic stages, when the SAC is known to be active (Figure 1A; Fischer *et al.*, 2004). We observed that the C-terminal kinase domain (amino acids 325–630) but not the N-terminal regulatory region (amino acids 1–332) localizes at kinetochores after expression of EGFP fusion proteins from transgenes under control of the normal *Mps1 cis*-regulatory region (Figure 1B). In contrast, the opposite behavior has been reported for the corresponding regions of human Mps1 (Liu *et al.*, 2003; Stucke *et al.*, 2004). However, consistent with the observations in human cells, a kinase-dead version (Mps1^{kd}, i.e., Mps1^{D478A}) tagged with EGFP displayed normal kinetochore localization (Figure 1B).

For the interpretation of kinetochore localization of mutant Mps1 versions, it is important to consider the role of endogenous wild-type Mps1. Human myc-Mps1 and GFP-Mps1 can be coimmunoprecipitated (Hewitt *et al.*, 2010), and additional evidence clearly supports Mps1–Mps1 interactions (Hached *et al.*, 2011; Lee *et al.*, 2012). Kinetochore localization of mutant Mps1 versions expressed in the presence of endogenous wild-type Mps1 might therefore reflect recruitment by the latter instead of binding to a distinct kinetochore-docking site. To determine whether *Drosophila* Mps1 also interacts in-*trans* with itself, we coexpressed myc-Mps1 and GFP-Mps1 in *Drosophila* S2R^{+} cells, followed by an analysis of coimmunoprecipitation (Supplemental Figure S1). These experiments clearly confirmed that *Drosophila* Mps1 dimerizes like human Mps1. Moreover, the C-terminal kinase domain but not the N-terminal regulatory region was found to associate with full-length Mps1 (Supplemental Figure S1). To determine whether kinase activity is required for this self-interaction in-*trans*, we coexpressed Mps1^{kd} versions tagged with myc and GFP. These Mps1^{kd} versions were ectopically expressed during larval stages where only a minor fraction of cells proliferate mitotically and express endogenous Mps1^{+} (Supplemental Figure S2A). The Mps1^{kd} versions expressed from heat-inducible transgenes were found to be coimmunoprecipitated with efficiency similar to that of wild-type Mps1 (Figure 1C). We conclude, therefore, that Mps1 protein kinase activity is not required for self-interaction in-*trans*.

On the basis of the observed self-interaction properties, it is possible that the localization of the C-terminal kinase domain of Mps1 and Mps1^{kd} to the kinetochore in wild-type embryos (Figure 1B) might reflect recruitment by endogenous Mps1. Moreover, Mps1 kinase activity has been implicated in the control of Mps1 kinetochore localization, although with some puzzling disagreement concerning the direction of its effect (Xu *et al.*, 2009; Colombo *et al.*, 2010; Hewitt *et al.*, 2010; Jelluma *et al.*, 2010). To evaluate whether endogenous wild-type Mps1 is required for the observed kinetochore localization of the mutant Mps1 versions, we expressed them in mutant embryos obtained from females with *Mps1*^{aldB4} germline clones. The *Mps1*^{aldB4} mutation results in a

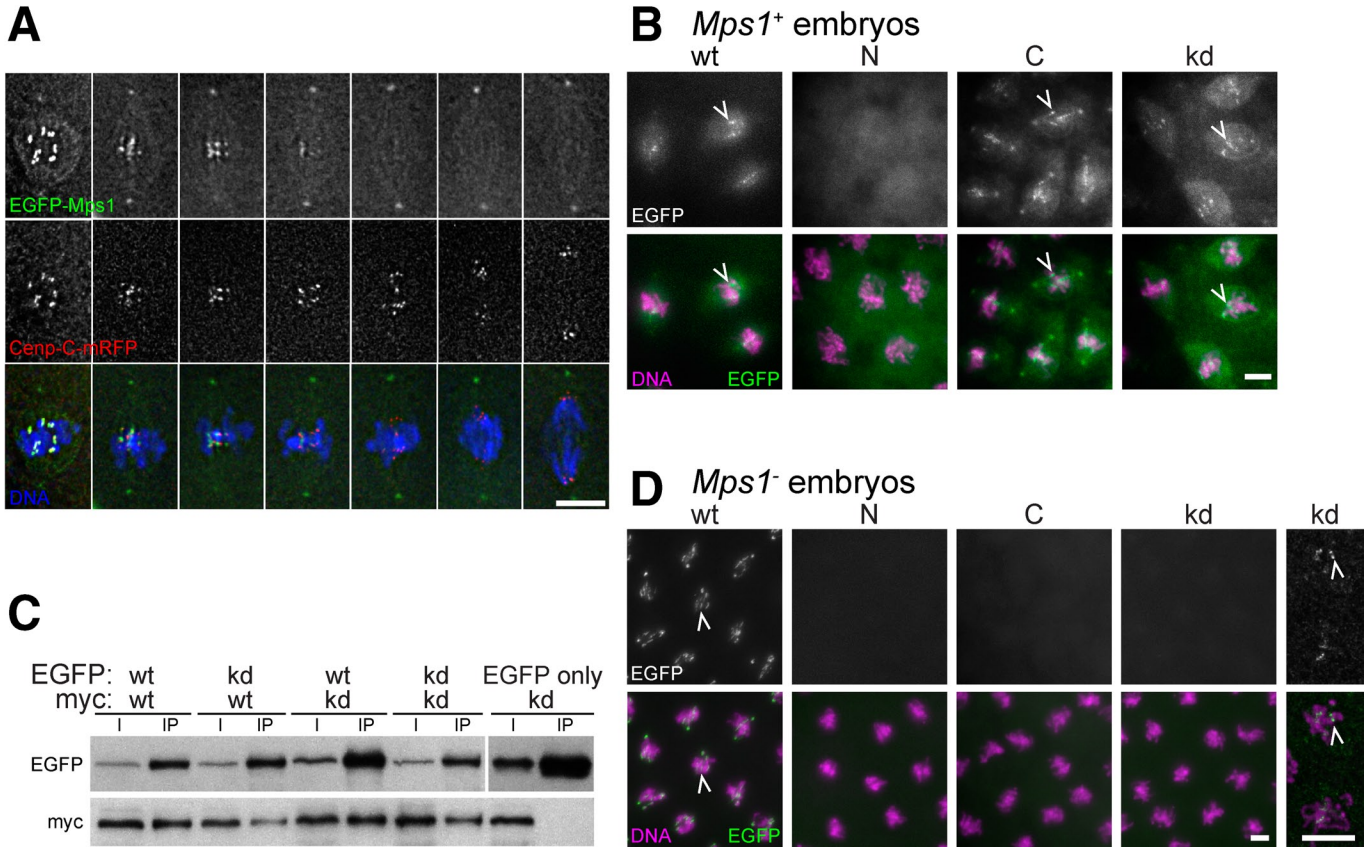

FIGURE 1: Localization and self-interaction of wild-type and mutant Mps1. (A) Mitotic figures from a mitotic wave in a syncytial-stage *Drosophila* embryo expressing EGFP-Mps1 and the centromere protein Cenp-C-mRFP after fixation and DNA labeling reveal peak levels of Mps1 at kinetochores during prometaphase (left), followed by disappearance from the kinetochore during progression into anaphase (right). EGFP-Mps1 is also detectable on centrosomes and weakly on the spindle. (B) Prometaphase figures from syncytial *Mps1*$^{+}$ embryos expressing the following EGFP-tagged Mps1 variants: wild-type (wt), N-terminal regulatory domain (N), C-terminal kinase domain (C), and kinase-dead Mps1^{kd} (kd). Arrowheads indicate kinetochore localization. (C) Larval extracts were used for immunoprecipitation with anti-EGFP after coexpression of an EGFP- and a myc-tagged Mps1 variant during a developmental stage with minimal endogenous Mps1 expression. Immunoblotting of extracts (I) and immunoprecipitates (IP) with anti-EGFP and anti-myc revealed coimmunoprecipitation of the tagged variants. Anti-EGFP does not coimmunoprecipitate myc-Mps1^{kd} from extracts of larvae expressing EGFP only instead of EGFP-Mps1, indicating the specificity of the Mps1 self-interaction. Loading was 1 and 15 larvae equivalents in I and IP lanes, respectively. (D) Prometaphase figures from syncytial *Mps1*$^{-}$ embryos expressing the EGFP-tagged Mps1 variants described in B. Arrowheads indicate kinetochore localization. In the case of EGFP-Mps1^{kd}, some residual kinetochore localization is only apparent after contrast enhancement (rightmost panels at higher magnification). Bars, 5 μm.

premature stop after the first 47 amino acids (Page *et al.*, 2007). Neither the N- nor the C-terminal Mps1 fragment localized to kinetochores in the *Mps1*^{aldB4}-mutant background (Figure 1D), even though these fragments were clearly expressed (Supplemental Figure S2B). In case of Mps1^{kd}, kinetochore signals were dramatically decreased (Figure 1D). Quantification of signal intensities revealed a reduction of Mps1^{kd} at prometaphase kinetochores to 2.5% when compared with wild-type Mps1 expressed analogously in the *Mps1*^{aldB4}-mutant background (698 arbitrary units [a.u.] ± 71, n = 25, for Mps1, vs. 17 a.u. ± 5, n = 26, for Mps1^{kd}). We conclude, therefore, that Mps1 kinase activity is required for kinetochore localization in *Drosophila*, in contrast to recent observations in mammalian cells (Hewitt *et al.*, 2010; Jelluma *et al.*, 2010; see *Discussion*). In case of the C-terminal domain of *Drosophila* Mps1, we cannot resolve whether its kinetochore localization in wild-type but not mutant background depends on recruitment by endogenous Mps1 or on Mps1 kinase activity.

Apart from kinetochore localization, the EGFP fusions of *Drosophila* Mps1, Mps1^{kd}, and Mps1^{C} (but not Mps1^{N}) were also detected at the centrosome throughout mitosis after expression in an *Mps1*$^{+}$ background (Figure 1, A and B). In the *Mps1*^{aldB4}-mutant background, only EGFP-Mps1 was detected at centrosomes (Figure 1C).

Mps1–Mad1 interactions

In an attempt to identify the elusive kinetochore component that provides the docking site for Mps1, proteins coimmunoprecipitated by EGFP-Mps1 were characterized by mass spectrometry. Apart from Mps1, we detected a number of highly abundant cellular proteins, reflecting nonspecific associations in all likelihood, and also Mad1/TXBP181-like (unpublished data). Immunoprecipitation (IP) Western experiments clearly confirmed the specificity of the Mps1–Mad1 interaction, which has also been observed in human cells (Lince-Faria *et al.*, 2009). From extracts of transgenic embryos,

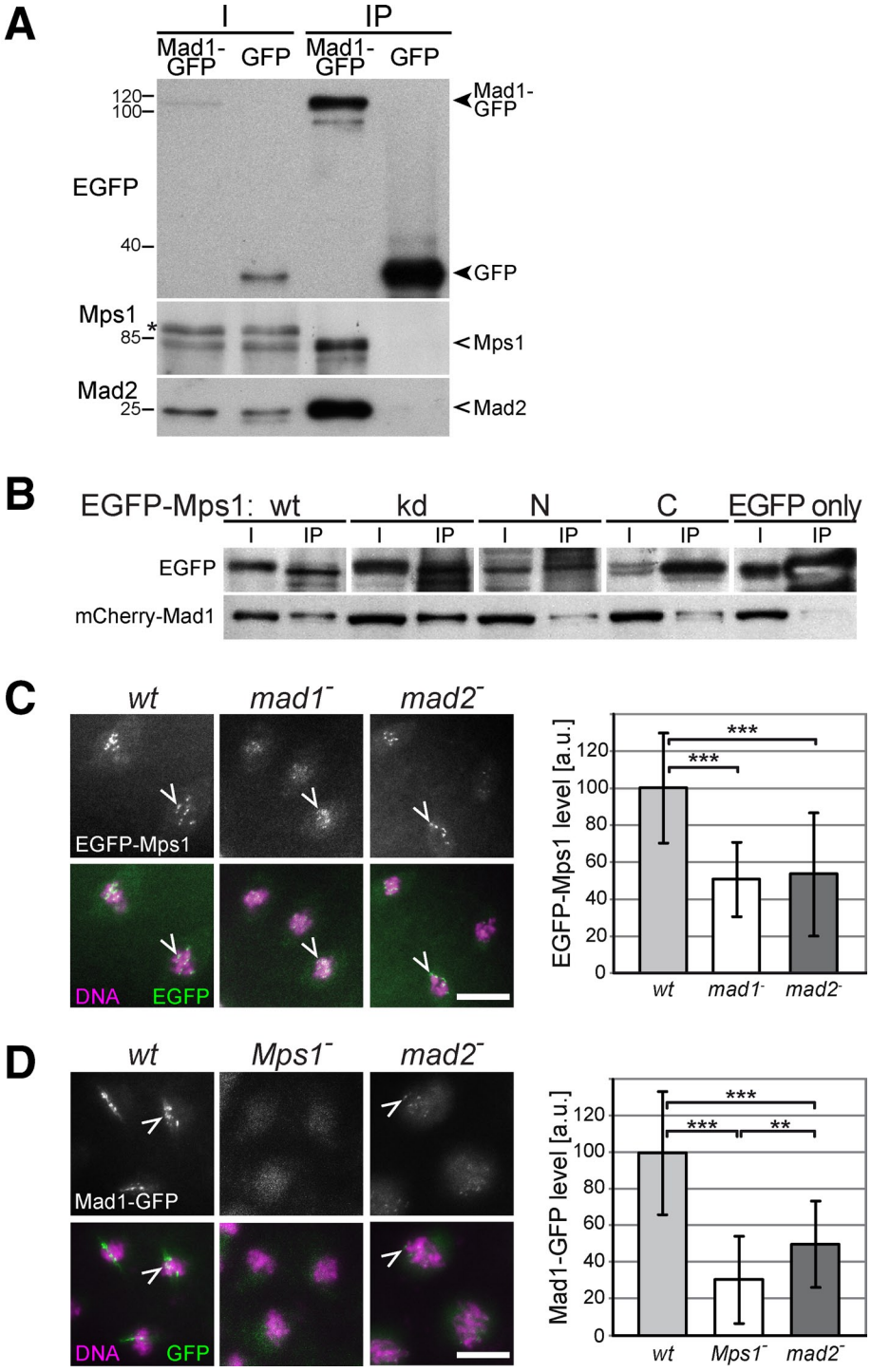

FIGURE 2: Mps1–Mad1 interaction and kinetochore localization dependences. (A) Extracts from embryos expressing either Mad1-GFP or GFP only were used for immunoprecipitation with anti-EGFP. Immunoblotting of extracts (I) and immunoprecipitates (IP) with anti-EGFP, anti-Mps1, and anti-Mad2 revealed that Mps1 and Mad2 are coimmunoprecipitated specifically with Mad1-EGFP. Loading was 30 and 925 embryo equivalents in I and IP lanes, respectively. The position of molecular weight markers is indicated on the left. A cross-reaction of anti-Mps1 is marked with an asterisk. (B) Extracts from embryos expressing mCherry-Mad1 and EGFP-tagged wild-type (wt), kinase-dead (kd), N-terminal (N), or C-terminal domain (C) of Mps1 were used for immunoprecipitation with anti-EGFP. Immunoblotting of extracts (I) and immunoprecipitates (IP) with anti-EGFP (EGFP) and anti-mCherry (mCherry-Mad1) indicated that all of the Mps1 variants associate with Mad1, although with reduced efficiency in case of the N- and C-terminal domains. However, even less mCherry-Mad1 was coimmunoprecipitated when EGFP only instead of an Mps1 fusion was expressed. Loading was 30 and 300 embryo equivalents in I and IP lanes, respectively. (C) Kinetochore localization of EGFP-Mps1 during prometaphase was analyzed in syncytial embryos from mothers that were wild type (*wt*), *mad1*$^{-}$, or *mad2*$^{-}$. (D) Kinetochore localization of Mad1-GFP during prometaphase was analyzed in syncytial embryos from mothers that were wild type (*wt*), *Mps1*$^{-}$, or *mad2*$^{-}$ (only in the germline in case of *Mps1*). Bars, 10 µm (C, D) . Arrowheads indicate kinetochore signals. Kinetochore signals were quantified (bar diagrams) using arbitrary units with error bars representing SD. Brackets indicate statistically significant differences (*t* test) with **$p < 0.01$ and ***$p < 0.001$.

Mad1-GFP pulled down not only Mad2, as expected (Chen *et al.*, 1999; Sironi *et al.*, 2002), but also Mps1 (Figure 2A). CoIP of Mps1 and Mad1-GFP was also observed after IP with anti-Mps1 instead of anti-GFP (unpublished data). Moreover, both the N- and the C-terminal domains of Mps1 were able to coimmunoprecipitate mCherry-Mad1, although less efficiently than full-length Mps1 and Mps1^{kd} (Figure 2B).

To determine whether Mad1 is required for Mps1 localization to kinetochores, we expressed EGFP-Mps1 in *mad1*^{1}/*Df(mad1)* mutants (Figure 2C). These mutants, which are viable and fertile, do not express Mad1 protein (Emre *et al.*, 2011). Loss of Mad1 resulted in a limited but significant decrease of EGFP-Mps1 on kinetochores according to our quantification during prometaphase of syncytial blastoderm mitoses (Figure 2C). Conversely, Mad1-GFP signals on kinetochores were found to be even more strongly dependent on the presence of Mps1. Apart from a weak, diffuse signal throughout the chromosome region, dot-like kinetochore signals were no longer apparent (Figure 2D). Although most reports from vertebrate cells clearly revealed a strong dependence of Mad1 kinetochore localization on both the presence and activity of Mps1 (Abrieu *et al.*, 2001; Martin-Lluesma *et al.*, 2002; Liu *et al.*, 2003; Vigneron *et al.*, 2004; Wong and Fang, 2006; Zhao and Chen, 2006; Jelluma *et al.*, 2008b; Tighe *et al.*, 2008; Hewitt *et al.*, 2010; Kwiatkowski *et al.*, 2010; Maciejowski *et al.*, 2010; Santaguida *et al.*, 2010; Sliedrecht *et al.*, 2010), quantitative data have not been published to our knowledge. Moreover, the partial dependence of Mps1 kinetochore localization on Mad1 in *Drosophila* embryos indicates that the Mps1–Mad1 interactions are not strictly hierarchical, and the partial reduction of both EGFP-Mps1 and EGFP-Mad1 on kinetochores in *mad2* mutants further emphasizes the complexity of the Mps1–Mad1–Mad2 interdependences.

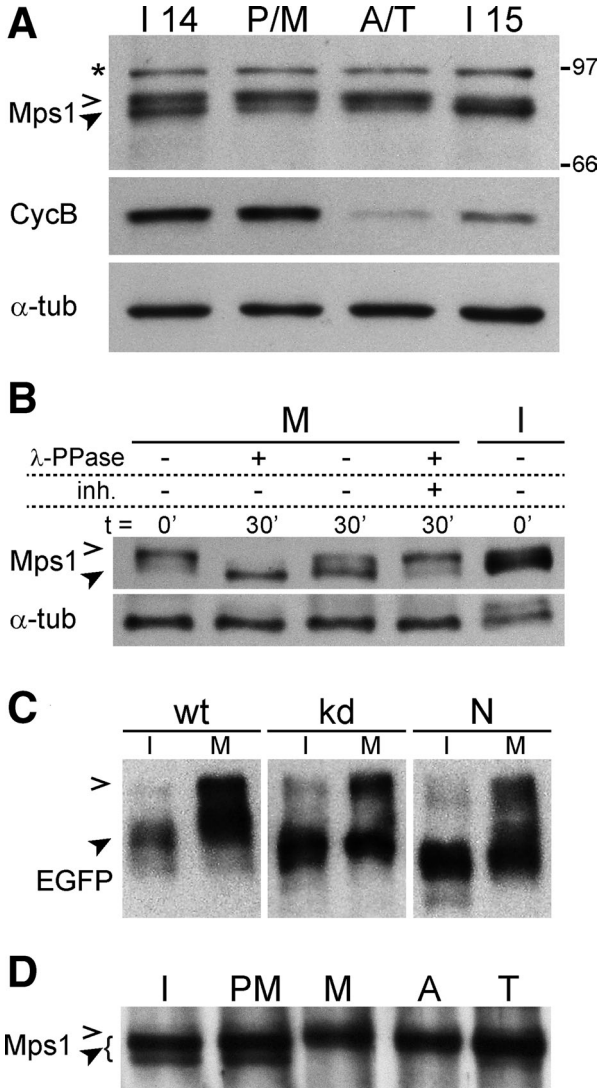

FIGURE 3: Mps1 stability and phosphorylation during mitosis. Progression through a synchronous mitosis 14 was induced in embryos. Extracts from microscopically selected embryos before mitosis (I14), in prophase and metaphase (P/M), in anaphase and telophase (A/T), and in the subsequent interphase (I15) were analyzed by immunoblotting with antibodies against Mps1, cyclin B, and α-tubulin (loading control) indicating that Mps1 levels do not decrease significantly during exit from mitosis. (B) Extracts from syncytial embryos in mitosis (M) or interphase (I) with (+) or without (–) pretreatment using λ-phosphatase (λ-PPase) and phosphatase inhibitors (inh.) for the indicated times were analyzed by immunoblotting with anti-Mps1 and anti–α-tubulin. (C) Extracts from *Mps1*-mutant embryos expressing EGFP-tagged wild-type (wt), kinase-dead (kd), or N-terminal domain (N) of Mps1 in interphase (I) or mitosis (M) were resolved on Phos-tag gels and analyzed by immunoblotting with anti-EGFP. (D) Extracts from microscopically selected syncytial embryos in interphase (I), prometaphase (PM), metaphase (M), anaphase (A), and telophase (T) were analyzed by immunoblotting with anti-Mps1. Open and filled arrowheads in A–D indicate phosphorylated low- and high-mobility forms of Mps1, respectively. A cross-reaction of anti-Mps1 is marked with an asterisk. Positions of molecular weight markers are indicated on the right.

Level and phosphorylation of Mps1 during progression through mitosis

The observed dependence of Mps1 kinetochore localization on Mad1 is relatively minor and unlikely to explain Mps1 localization dynamics during mitosis. However, APC/C-mediated degradation of Mps1 during exit from mitosis has been implicated in Mps1 regulation in yeast and human cells (Palframan *et al.*, 2006; Cui *et al.*, 2010). To analyze the total levels of *Drosophila* Mps1 during progression through mitosis, we applied a highly efficient synchronization procedure, including microscopic isolation of embryos in precisely defined mitotic stages. Immunoblotting did not reveal a difference in Mps1 levels before and after the metaphase-to-anaphase transition, whereas cyclin B amounts decreased dramatically, as expected (Figure 3A). We conclude, therefore, that disappearance of *Drosophila* Mps1 from kinetochores during exit from mitosis does not reflect overall degradation, as also suggested by similar, although less accurately staged analyses from vertebrates (Stucke *et al.*, 2002; Liu *et al.*, 2003; Grimison *et al.*, 2006; Sun *et al.*, 2010).

Immunoblotting with anti-Mps1 revealed multiple isoforms in embryo extracts (Figure 3A), suggesting that *Drosophila* Mps1 is a phosphoprotein as previously observed in other organisms (Stucke *et al.*, 2002; Grimison *et al.*, 2006; Palframan *et al.*, 2006; Zhao and Chen, 2006). Phosphatase treatment converted the isoforms with low electrophoretic mobility, which were predominant in M phase, into a faster-migrating species (Figure 3B), demonstrating that *Drosophila* Mps1 is hyperphosphorylated during mitosis. The corresponding phosphorylation sites are present in the N-terminal region, since only the N- but not the C-terminal region displayed decreased electrophoretic mobility during mitosis (unpublished data).

Autophosphorylation of human Mps1 is known to be required for full kinase activity and SAC function in vivo (Kang *et al.*, 2007; Mattison *et al.*, 2007; Jelluma *et al.*, 2008b; Wang *et al.*, 2009). To evaluate whether the observed hyperphosphorylation of *Drosophila* Mps1 reflects autophosphorylation, we expressed different EGFP-Mps1 variants in an *Mps1*-null mutant background and compared their electrophoretic mobility in interphase and mitosis after resolution of extracts on Phos-tag gels (Kinoshita *et al.*, 2009). EGFP-Mps1^{kd} and the N-terminal Mps1 region displayed a mobility shift in M phase similar to that of the wild-type version (EGFP-Mps1; Figure 3C). Therefore we conclude that protein kinases other than Mps1 are involved in mitotic hyperphosphorylation of Mps1.

Mitogen-activated protein kinase (MAPK) phosphorylates Mps1 in *Xenopus*, allowing kinetochore localization of Mps1 and other checkpoint proteins (Zhao and Chen, 2006). To analyze whether mitotic Mps1 hyperphosphorylation in *Drosophila* is temporally correlated with its localization on the kinetochore, we performed immunoblotting with extracts prepared from microscopically staged syncytial embryos, where thousands of nuclei progress synchronously through mitosis. In this manner, hyperphosphorylation was found to perdure to late mitotic stages (Figure 3D) when Mps1 is no longer detected on kinetochores and the SAC is inactive. We conclude that the mitotic phosphorylation that causes the Mps1 electrophoretic mobility shift is unlikely to be sufficient for Mps1 kinetochore localization and SAC activation.

Precise control of Mps1 localization and level is crucial for normal mitosis

Although the molecular basis for the disappearance of Mps1 from kinetochores during metaphase is not understood in detail, elegant experiments in human cells recently demonstrated that this process is crucial for SAC silencing and progression from metaphase into anaphase (Jelluma *et al.*, 2010). In these experiments, the normal disappearance of Mps1 from kinetochores was prevented by expression of an Mps1 variant fused to Mis12, a kinetochore component that is present throughout mitosis. Recently similar experiments with an Mps1 variant fused to Ndc80 kinetochore protein

were performed in fission yeast (Ito *et al.*, 2012). In independently initiated work, we applied the same experimental strategy, although with different constitutive kinetochore targeting domains. We fused the C-terminal domain of *Drosophila* Cenp-C, which is sufficient for kinetochore localization (Heeger *et al.*, 2005), and EGFP to Mps1. Apart from this EGFP-CenpC^{C}-Mps1 fusion (EC-Mps1), we also expressed a kinase-dead variant (EC-Mps1^{kd}) during interphase 14 of *Drosophila* embryogenesis (using the UAS/GAL4 system). When EC-Mps1^{kd} was expressed, we did not observe abnormalities during progression through the subsequent mitosis 14 (Figure 4, A and B). In particular, we emphasize that anaphase and telophase figures were normal, that is, without chromatin bridges. Of importance, GFP but not anti-BubR1 signals were clearly detected at kinetochores during these late mitotic stages, indicating that at least a fraction of EC-Mps1^{kd} indeed persists at the kinetochore throughout mitosis, as expected (Figure 4B). This localized fraction is evidently not sufficiently abundant to outcompete endogenous Cenp-C to an extent incompatible with normal mitosis. However, 10-fold-higher expression levels, as determined by quantitative immunoblotting, of only the EC part without Mps1 resulted in mitotic defects, as expected from a dominant-negative effect on Cenp-C (unpublished data; Heeger *et al.*, 2005).

In contrast to EC-Mps1^{kd}, expression of EC-Mps1 caused severe mitotic defects (Figure 4, A and B). Unexpectedly, however, EC-Mps1 did not cause an extended mitotic delay or arrest in metaphase, as predicted if persistent SAC activation was induced. Prophase and metaphase figures were normal in number and appearance. In contrast, cells in anaphase, telophase, and early in the next interphase displayed chromatin bridges (Figure 4, A and B). Centromeric EC-Mps1 signals were observed near these bridges (Figure 4B), indicating a failure of sister kinetochore segregation to spindle poles.

The chromosome segregation defects were obtained after EC-Mps1 expression in embryos with endogenous Mps1. An overall increase in Mps1 levels rather than persistent kinetochore localization might therefore explain the observed defects. To analyze whether excess Mps1 causes mitotic defects, we expressed E-Mps1 (lacking the Cenp-C^{C} localization domain) on top of endogenous Mps1. Strikingly, this resulted in a pronounced mitotic delay during metaphase, as evidenced by a strong enrichment of metaphase figures in fixed embryos (Figure 4A). On the one hand, this result was unexpected. Metaphase delays were not observed in our earlier experiments with *Drosophila* strains having extra *Mps1*$^{+}$ gene copies (Fischer *et al.*, 2004). Similarly, *Mps1/Ttk* overexpression in mammalian cells does not result in mitotic delays (Stucke *et al.*, 2002; Kang *et al.*, 2007). On the other hand, *MPS1* overexpression in budding yeast is clearly sufficient for SAC activation and mitotic arrest (Hardwick *et al.*, 1996). The overexpression applied here resulted in E-Mps1 levels that were about fivefold higher than those of endogenous Mps1 (Figure 4C). Threefold instead of fivefold excess obtained with a weaker transgene insertion was insufficient to cause the same strong metaphase delays (Supplemental Figure S3).

High levels of E-Mps1^{kd} expression did not result in metaphase enrichment or other mitotic defects (Figure 4A and Supplemental Figure S3), indicating that the metaphase delay caused by high levels of E-Mps1 depends on Mps1 kinase activity. Our quantitative immunoblotting experiments also showed that the expression level of EC-Mps1 was below the E-Mps1 level that caused a metaphase delay (Figure 4D), suggesting that EC-Mps1 is a relatively unstable variant.

Kinetochore levels observed after EC-Mps1 and E-Mps1 overexpression were quantified microscopically (Supplemental Figure S4). E-Mps1 kinetochore levels were found to be approximately twofold increased in prometaphase. The overwhelming majority of metaphase cells had such high levels of overexpressed E-Mps1 at kinetochores. In contrast, without overexpression E-Mps1 signals disappear rapidly from kinetochores during metaphase. In anaphase cells, E-Mps1 was no longer detectable on kinetochores even after overexpression. Overexpression of EC-Mps1 resulted in a more limited increase at kinetochores in prometaphase (~1.8-fold), but these kinetochore signals were largely maintained during exit from mitosis (70% of prometaphase signal intensity during anaphase/telophase).

In summary, EC-Mps1, which persists at kinetochores throughout mitosis, caused chromosome segregation defects (but not a substantial metaphase delay) at an expression level comparable to that of endogenous wild-type Mps1, whereas E-Mps1 resulted in a different mitotic abnormality, that is, a strong metaphase delay, but only after approximately fivefold overexpression. Therefore we conclude that normal exit from mitosis in *Drosophila* depends critically on both normal localization and normal levels of Mps1.

Apart from Mps1, Bub1, BubR1, and Mad2 play prominent roles in the SAC. Similar to Mps1, these proteins also accumulate on kinetochores during prometaphase and decrease again after chromosome attachment to the spindle before anaphase onset also in *Drosophila* (Basu *et al.*, 1999; Logarinho *et al.*, 2004; Buffin *et al.*, 2005). To evaluate whether localization and levels of these proteins are equally critical as in the case of Mps1, we performed analogous experiments. However, expression of *E-Bub1* and *E-BubR1*, as well as an *E-BubR1* version fused to the constitutive Cenp-C^{C} localization domain, did not perturb progression through mitosis in *Drosophila* embryos (Supplemental Figure S5). In addition, *E-mad2* overexpression did not cause mitotic abnormalities (Supplemental Figure S5).

The mitotic defects observed after enforcing persistent Mps1 maintenance at the kinetochore by *EC-Mps1* expression in *Drosophila* embryos are different from those caused by Mis12-Mps1 in human cells, possibly because of localization differences. The positions of the Cenp-C^{C} domain and of Mis12 within the kinetochore have been determined accurately along the spindle axis by super-resolution (Schittenhelm *et al.*, 2007), and Mps1 has been localized at the ultrastructural level (Dou *et al.*, 2003). Accordingly, Mps1 is normally located within the outer corona, whereas Mis12 is further inward and Cenp-C^{C} even more so. In an attempt to enforce Mps1 persistence at a kinetochore location that is as close as possible to normal, we performed experiments with an E-Mps1-Nuf2 fusion, which is predicted to localize Mps1 at the base of the outer corona (DeLuca *et al.*, 2005; Schittenhelm *et al.*, 2007). E-Mps1-Nuf2 expression resulted in metaphase delays. However, this observation cannot be viewed as support for the notion that Mps1 disappearance from the kinetochore is required for SAC silencing because most of the overexpressed E-Mps1-Nuf2 protein did not appear to be localized at the kinetochore, and overall this fusion protein was not more effective in causing metaphase delays than E-Mps1 (Supplemental Figure S6). Similarly, an experiment to address the effect of Mps1 dimerization after ectopic targeting to the cell membrane (Tor-E-Mps1 and Tor^{4021}-E-Mps1) remained inconclusive because of technical complications (Supplemental Figure S6).

Excess Mps1 inhibits sister chromatid separation independent of the SAC

To characterize the metaphase delay resulting from excess Mps1 in further detail, we performed time-lapse in vivo imaging with embryos expressing fluorescent proteins for visualization of chromosomes, kinetochores, and spindles (combinations of histone H2Av–monomeric red fluorescent protein [mRFP] and Cenp-A/Cid-EGFP or Tomato-Cenp-C and Jupiter-GFP; Figure 5). These experiments

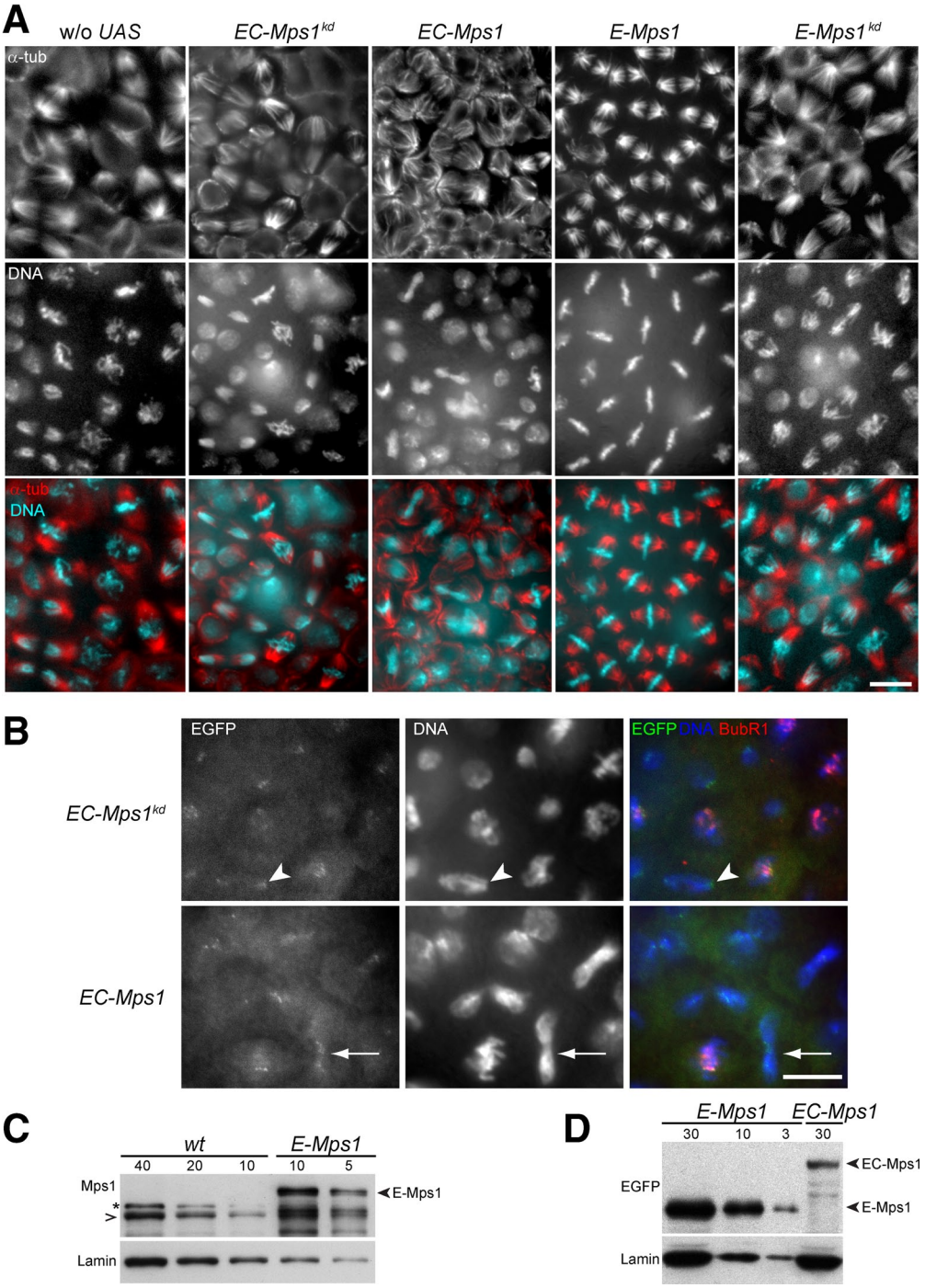

FIGURE 4: Mitotic defects caused by alterations in localization and level of Mps1. The UAS/GAL4 system was used for expression of Mps1 variants in embryos before mitosis 14. (A, B) Embryos were fixed at the stage of mitosis 14. The epidermal regions with mitotic domain 10 (Foe, 1989) are displayed after labeling with anti-α-tubulin (α-tub, A), anti-BubR1 (BubR1, B), and a DNA stain (DNA, A and B). As in control embryos without a *UAS* transgene (w/o *UAS*), progression through mitosis 14 was normal after expression of kinase-dead *EGFP-Cenp-C^{C}-Mps1^{kd}* (*EC-Mps1^{kd}*), which localizes to kinetochores beyond metaphase, as indicated by EGFP signals on kinetochores in anaphase (arrowhead in B). However, chromosome segregation defects during completion of mitosis were apparent after expression of *EGFP-Cenp-C^{C}-Mps1* (*EC-Mps1*), as revealed by DNA bridges with EGFP signals in anaphase and telophase figures (arrow in B). Whereas a strong delay in metaphase was observed after overexpression of *EGFP-Mps1* (*E-Mps1*), progression through mitosis 14 was normal after overexpression of *EGFP-Mps1^{kd}* (*E-Mps1^{kd}*). Bars, 10 μm. (C, D) Expression levels of the Mps1 variants at the stage analyzed in A and B were determined by quantitative immunoblotting with antibodies against Mps1, EGFP, and lamin as loading control. Serial dilutions of embryo extracts were loaded with numbers representing embryo equivalents. (C) Compared to Mps1 in wild-type embryos (*wt*), EGFP-Mps1 (*E-Mps1*) levels were approximately fivefold higher. (D) Compared to EGFP-Mps1, EGFP-Cenp-C^{C}-Mps1 (*EC-Mps1*) levels were ~10-fold lower. A cross-reaction of anti-Mps1 is marked with an asterisk. The positions of wild-type Mps1 and EGFP fusions are indicated by open and filled arrowheads, respectively.

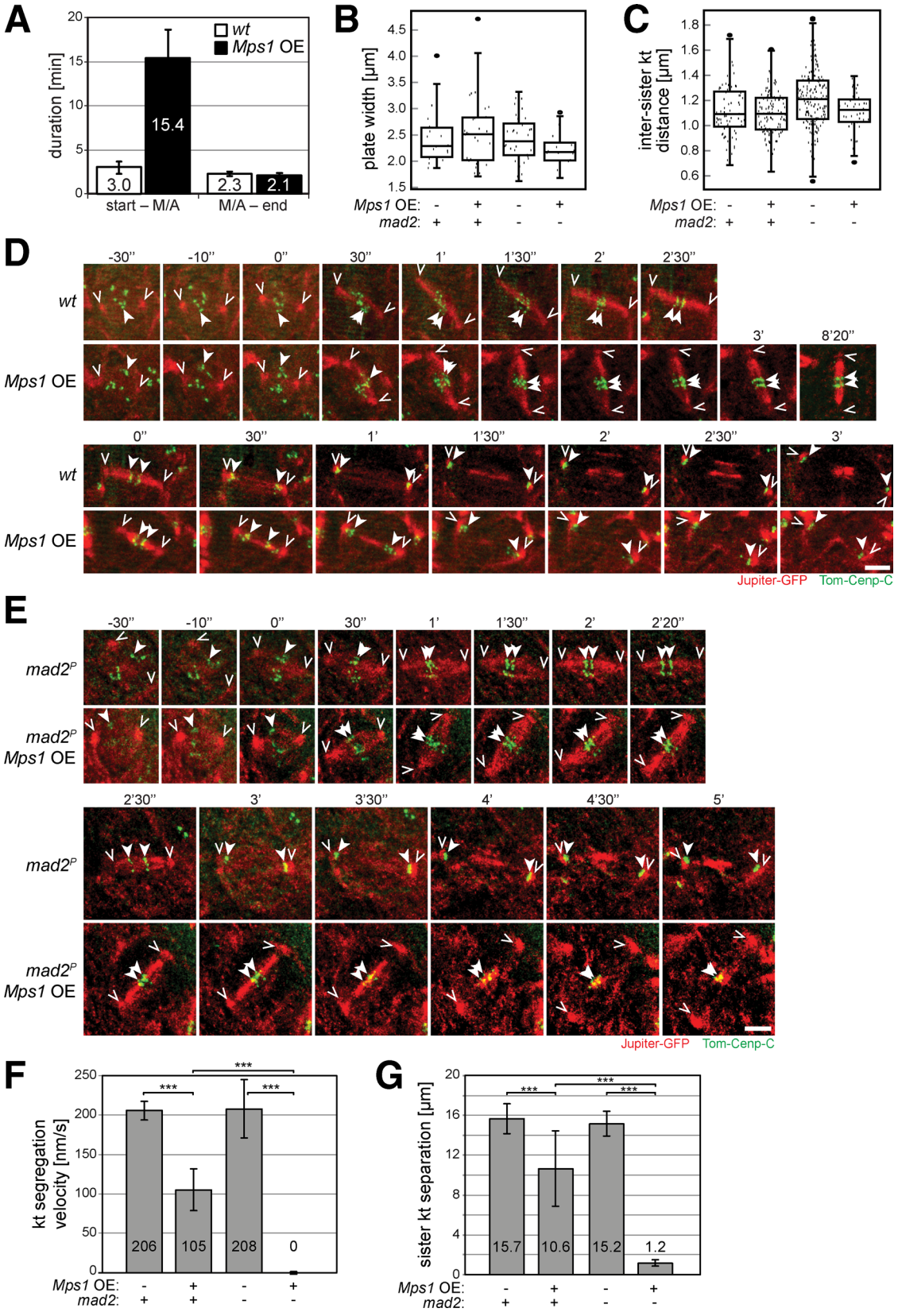

FIGURE 5: SAC effects on mitosis in presence of excess Mps1. (A) The dynamics of progression through mitosis 14 was analyzed by time-lapse in vivo imaging of embryos without (wt, white bars) or with UAS/GAL4-mediated *Mps1* overexpression (*Mps1* OE, black bars). Because embryos also expressed histone H2Av-mRFP and the centromere protein Cenp-A/Cid-EGFP, the duration from prophase onset until metaphase-to-anaphase transition (start–M/A), as well as from metaphase-to-anaphase transition until telophase end (M/A– end), could be determined. Bars indicate average duration (±SD) obtained from >50 mitotic cells from at least six different embryos. (B, C) The width of metaphase plates

confirmed that excess Mps1 delayed mitotic progression in metaphase. Although chromosome condensation and congression into the metaphase plate appeared to proceed with the same speed as in control embryos, metaphase was ~10 times longer after *Mps1* overexpression. Thereafter, completion of mitosis occurred with similar kinetics as in controls (Figure 5, A and D).

Yeast and human Mps1 are known to destabilize erroneous kinetochore attachments to spindle microtubules (Jones *et al.*, 2005; Maure *et al.*, 2007; Jelluma *et al.*, 2008b; Tighe *et al.*, 2008; Hewitt *et al.*, 2010; Maciejowski *et al.*, 2010; Santaguida *et al.*, 2010; Sliedrecht *et al.*, 2010). In *Drosophila*, accordingly, the delay of the metaphase-to-anaphase transition might be caused by excess Mps1 via a primary effect on kinetochore attachment and consequent secondary SAC activation. To evaluate this possibility, we analyzed metaphase plate formation. A general impairment of kinetochore attachment as a result of excess Mps1 is expected to result in a widening of the metaphase plate. Therefore we compared the width of metaphase plates in *Mps1*-overexpressing and control embryos 2 min after nuclear envelope breakdown (NEBD), that is, at a time point that is ~30 s before anaphase onset in control embryos. Metaphase plates are expected to be widened if some or all chromosomes fail to congress into the metaphase plate (Oliveira *et al.*, 2005). However, we failed to observe a significant difference (Figure 5B). Moreover, we also measured the separation between sister kinetochores, which is known to respond to physical tension resulting from biorientation. In *Drosophila* embryos, the separation between sister kinetochores in chromosomes with normal bipolar attachment is ~1.6-fold higher than with unattached chromosomes (Heeger *et al.*, 2005; Pandey *et al.*, 2007). However, we were unable to detect a significant difference in the average sister kinetochore distance when comparing *Mps1*-overexpressing and control embryos 2 min after NEBD (Figure 5C).

On the basis of our analysis of metaphase plate width and sister kinetochore separation, it did not appear that excess Mps1 caused the observed mitotic delay via destabilization of kinetochore attachments. Therefore we considered the possibility that excess Mps1 might activate the SAC directly without affecting primarily spindle dynamics and/or kinetochore attachment. Accordingly, blocking SAC function downstream of Mps1 is expected to restore a largely normal progression through mitosis in *Mps1*-overexpressing embryos because the SAC is known to be dispensable for mitosis in *Drosophila* (Buffin *et al.*, 2007). Therefore we compared progression through mitosis in *mad2*-null mutants (*mad2*^{P}) (Buffin *et al.*, 2007) in the presence and absence of *Mps1* overexpression (Figure 5E). In *mad2* mutants, excess Mps1 no longer resulted in a metaphase delay. We conclude, therefore, that the pause in metaphase caused by *Mps1* overexpression in the presence of *mad2*$^{+}$ function depends on SAC activity.

Although mitosis was no longer delayed after *Mps1* overexpression in *mad2*-mutant embryos, the completion of mitosis was surprisingly abnormal. Chromosome movement during anaphase was almost completely abolished (Figure 5, E–G). Scoring of the metaphase-to-anaphase transition was therefore based on spindle appearance, which displayed a sudden although limited extension. In contrast, without excess Mps1, anaphases were mostly normal in *mad2*-mutant embryos (Figure 5, F and G).

The severe failure of chromosome segregation during anaphase resulting from *Mps1* overexpression in *mad2*-mutant embryos prompted us to measure metaphase plate width and sister kinetochore separation also in these embryos. These measurements were performed 2 min after NEBD as previously in the *mad2*$^{+}$ background. We did not detect statistically significant differences, indicating that also in the *mad2*-mutant background *Mps1* overexpression did not interfere with chromosome alignment into the metaphase plate. The failure of chromosome segregation during anaphase in *mad2*-mutant embryos with excess Mps1 therefore is very unlikely to reflect a lack of stable bipolar sister kinetochore attachment.

Like Mps1, BubR1 is also present at maximal levels at unattached kinetochores in prometaphase and strongly diminished in metaphase (Taylor *et al.*, 2001). Moreover, it was proposed that BubR1 levels at kinetochores are inversely correlated with physical tension (Skoufias *et al.*, 2001; Logarinho *et al.*, 2004). Therefore we analyzed the behavior of BubR1-GFP after *Mps1* overexpression in *mad2*$^{+}$ and *mad2*$^{-}$ embryos (Figure 6). The rapid initial accumulation of BubR1-GFP on kinetochores after entry into mitosis reached peak levels in prometaphase and was not affected by *Mps1* overexpression (Figure 6, A, C, and D). Moreover, *Mps1* overexpression did also not affect the initial phase of the subsequent disappearance of BubR1-GFP from kinetochores during metaphase in both *mad2*$^{+}$ and *mad2*$^{-}$ embryos (Figure 6, B–D). However, the late phase of BubR1-GFP disappearance from kinetochores was slowed down by *Mps1* overexpression (Figure 6, B–D), in particular from one or two exceptional kinetochores within a given metaphase cell (Figure 6B). At the time of the metaphase-to-anaphase transition BubR1-GFP signals were no longer detectable on kinetochores. These observations suggest that *Mps1* overexpression might result in transient detachment of one or two occasional kinetochores, causing SAC activation and metaphase delay in *mad2*$^{+}$ embryos. However, the observed BubR1-GFP behavior argues strongly against the interpretation that the

(B) and separation of sister kinetochores (C) was determined after in vivo imaging of mitosis 14 in embryos expressing the centromere protein Tomato-Cenp-C and the spindle-associated protein Jupiter-GFP (see also D and E). Moreover, embryos were either *mad2*$^{+}$ (+) or *mad2*$^{-}$ (–) and did (+) or did not (–) overexpress *Mps1* (*Mps1* OE). Box plots display values determined 2 min after nuclear envelope breakdown. The *t* tests failed to reveal significant differences between the different genotypes. (D, E) Entry into mitosis 14 until metaphase (top) and exit from mitosis 14 (bottom) was analyzed by in vivo imaging of embryos with the same genotypes as in B and C. Comparison of *mad2*$^{+}$ embryos (D) either without (*wt*) or with *Mps1* overexpression (*Mps1* OE) indicated that excess Mps1 resulted in a substantial metaphase delay, eventually followed by almost normal sister chromatid segregation during anaphase. In contrast, comparison of *mad2*$^{-}$ embryos (E) either without (*wt*) or with *Mps1* overexpression (*Mps1* OE) revealed that the metaphase delay induced by excess Mps1 depends on SAC function. Moreover, sister chromatid segregation was almost completely inhibited during exit from mitosis in *mad2*$^{-}$ embryos with excess Mps1. Maximum projections of selected stacks at the indicated times are shown from representative cells with spindle poles indicated by open and kinetochores by closed arrowheads. Bars correspond to 5 µm. (F, G) The speed of poleward sister kinetochore segregation during anaphase (F) and their final separation at the end of mitosis (G) in embryos with the same genotypes as in B–E were quantified. Bars represent average (±SD) from 12 mitotic cells from at least three embryos. Brackets indicate statistically significant differences (*t* test) with ***$p < 0.001$.

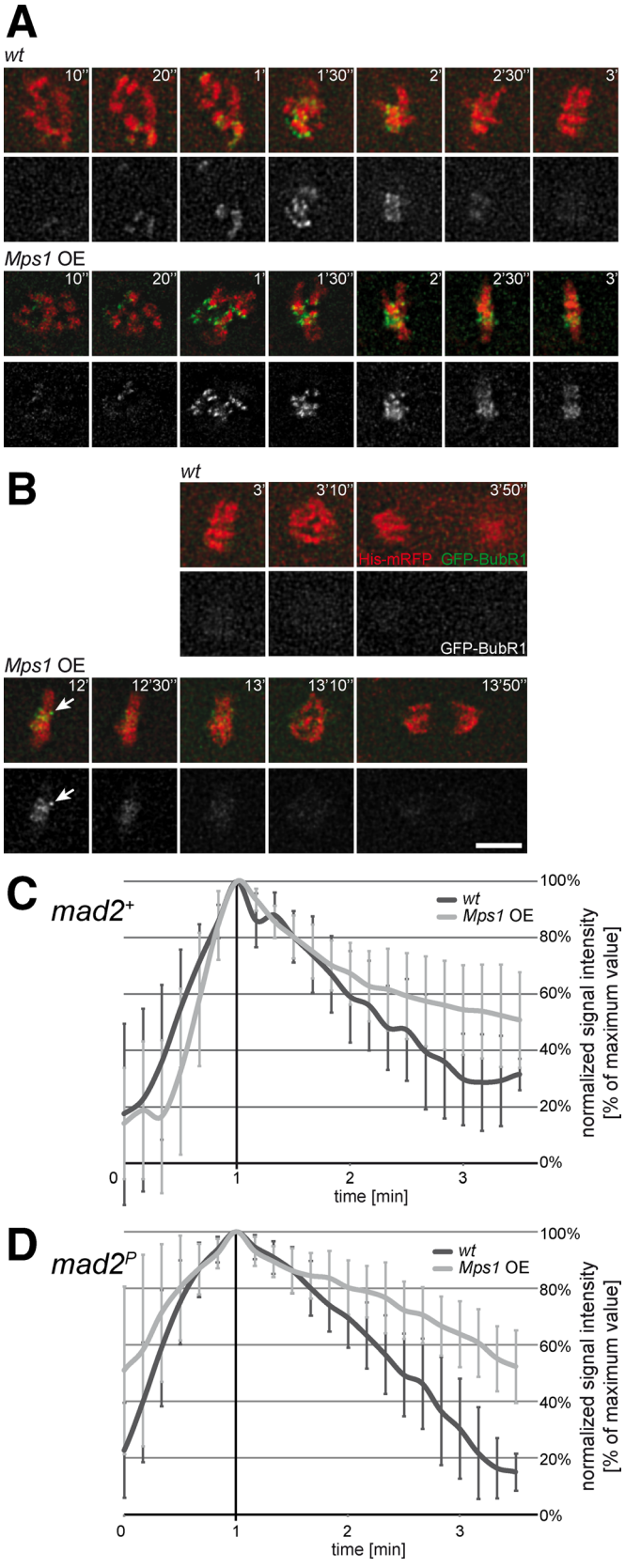

FIGURE 6: BubR1 kinetochore localization during mitosis in presence of excess Mps1. (A–C) Embryos with GFP-BubR1 and histone H2Av-mRFP either without (*wt*) or with UAS/GAL4-mediated *Mps1* overexpression (*Mps1* OE) were analyzed by time-lapse in vivo imaging. Maximum projections of selected stacks at the indicated times are shown from representative cells during (A) entry into mitosis and (B) exit from mitosis. Arrow indicates a single kinetochore retaining GFP-BubR1 during the metaphase delay induced by excess Mps1. Bar, 5 µm. (C) GFP-BubR1 signals on kinetochores were quantified over time, and curves were aligned at their peak and averaged (±SD). Although accumulation and subsequent initial disappearance of BubR1 from kinetochores was not affected by excess Mps1, this overexpression led to a slowdown of the late phase of BubR1 disappearance, presumably due to the one or two GFP-BubR1–retaining kinetochores characteristically observed during the metaphase delay caused by excess Mps1. (D) GFP-BubR1 signals on kinetochores were also analyzed in *mad2*-mutant embryos either without (*wt*) or with UAS/GAL4-mediated *Mps1* overexpression (*Mps1* OE). As in *mad2*$^{+}$ embryos (A–C), excess Mps1 did not affect accumulation and subsequent initial disappearance of BubR1 from kinetochores.

severe anaphase defects caused by *Mps1* overexpression in *mad2*$^{-}$ embryos reflect a global inability to form stable kinetochore attachments. The large majority of chromosomes appear to undergo normal attachment and biorientation also after *Mps1* overexpression.

To determine whether *Mps1* overexpression also abolished chromosome segregation during anaphase when SAC function was impaired by mutations other than *mad2*^{P}, we performed analogous experiments in *bubR1*^{KEN} mutants. These mutants are also characterized by a complete loss of SAC function (Rahmani *et al.*, 2009). *Mps1* overexpression in these mutants was found to cause the same anaphase defects as in *mad2* mutants (unpublished data).

If not insufficient kinetochore attachment, what else might cause the severe chromosome segregation defects during anaphase in the presence of excess Mps1 in SAC-deficient embryos? It is intriguing that *Mps1* overexpression affected anaphase far less drastically in *mad2*$^{+}$ than in *mad2*$^{-}$ embryos. In *mad2*$^{+}$ embryos, *Mps1*-overexpressing cells eventually entered anaphase and completed mitosis. Sister chromatids were far more effectively transported poleward than in *Mps1*-overexpressing *mad2*-mutant embryos. Nevertheless, the speed and extent of chromosome separation were not entirely normal in comparison to control embryos without *Mps1* overexpression (Figure 5, F and G). Anaphase quality, as well as overall survival of embryos, was dependent not only on *mad2* function, but also to some extent on the particular combination of fluorescent marker proteins (Supplemental Figure S7). The different marker proteins (histone H2Av-mRFP, Cenp-A/Cid-EGFP, Tomato-Cenp-C, and Jupiter-GFP) might well have weak SAC-activating effects to variable degrees. All our observations were therefore consistent with the interpretation that SAC-dependent pausing in metaphase counteracts the negative effects of excess Mps1 on chromosome segregation during anaphase. Accordingly, we hypothesized that cohesion fatigue during metaphase extensions might oppose a SAC-independent Mps1 effect on sister chromatid resolution. Cohesion fatigue has been described recently in human cells, where spindle forces can, with time, rupture normal sister chromatid cohesion during extended metaphase arrest (Daum *et al.*, 2011; Stevens *et al.*, 2011). The efficiency of sister chromatid resolution might not be sufficient to allow poleward chromatid segregation after cohesion stabilization by excess Mps1, when anaphase is initiated early, as in *mad2*-mutant embryos (Figure 7E). However, after delayed anaphase onset, as in *mad2*$^{+}$ embryos, sister chromatid resolution might be efficient enough to allow some segregation because cohesion fatigue might have canceled out the stabilizing effect of excess Mps1 on sister chromatid cohesion (Figure 7D).

Our hypothesis that excess Mps1 might lead to stabilization of sister chromatid cohesion in a SAC-independent manner predicts

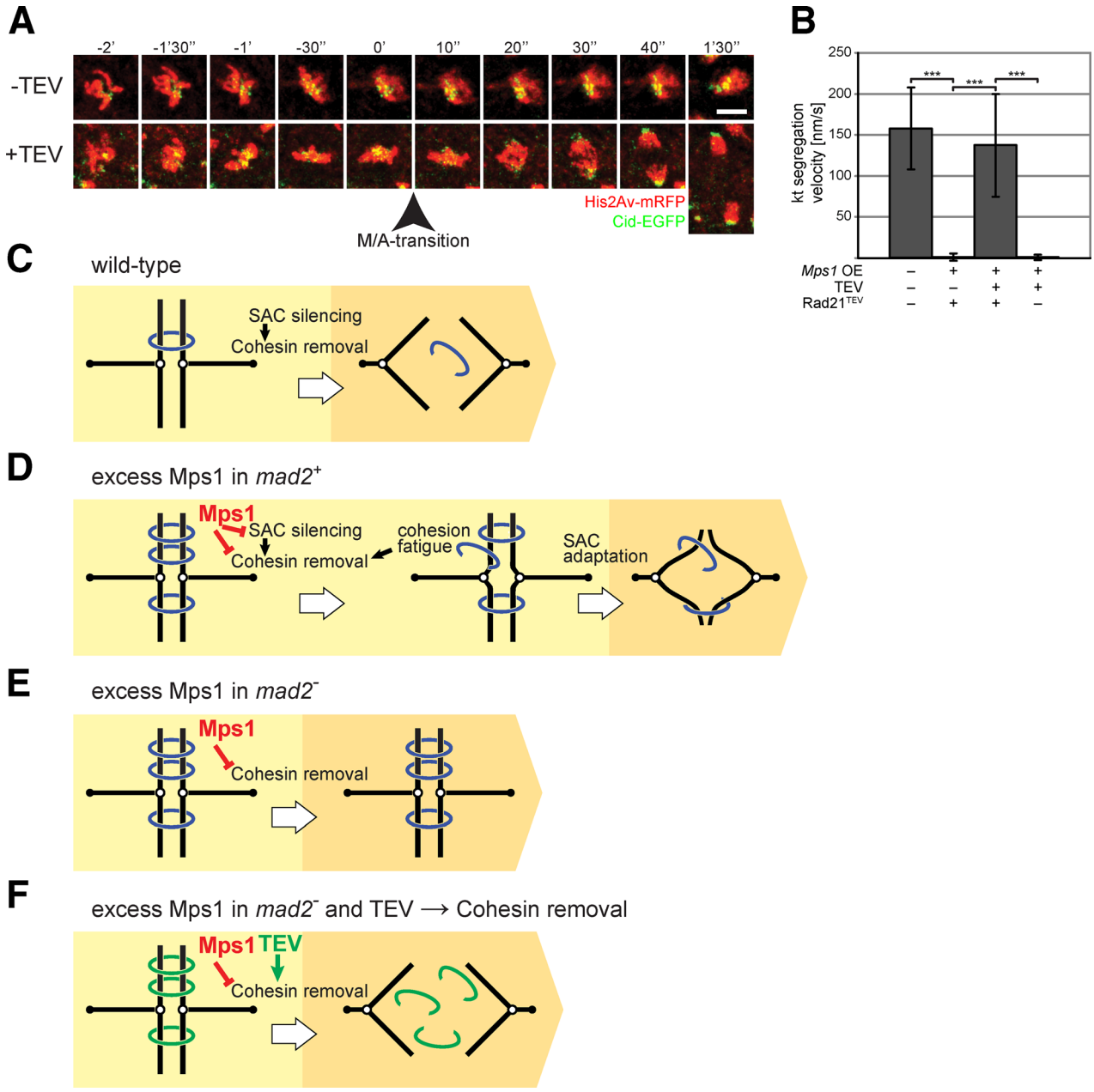

FIGURE 7: SAC-independent inhibition of sister chromatid separation by excess Mps1. (A, B) The UAS/GAL4 system was used for *Mps1* overexpression in *mad2*-mutant embryos before mitosis 14. These embryos also expressed histone H2Av-mRFP and Cid-EGFP, allowing in vivo imaging of progression through mitosis 14. Moreover, instead of the wild-type cohesin subunit Rad21, these embryos expressed a Rad21 version with inserted internal TEV protease cleavage sites. In the presence of a *UAS-TEV* transgene, therefore, separase-independent cleavage of Rad21 occurred, resulting in elimination of sister chromatid cohesion (Pauli *et al.*, 2008). (A) Maximum projections of selected stacks at the indicated times from representative cells of embryos without (–TEV) or with *UAS-TEV* (+TEV) reveal that TEV expression restores an essentially normal poleward sister chromatid segregation during anaphase in the presence of excess Mps1. Bar, 5 µm. (B) Quantification of the velocity of poleward sister chromatid segregation during anaphase in *mad2*^{P} *His2Av-mRFP Cid-EGFP* embryos with maternally derived Gal4 and variable aspects of the genotype (*UAS-Mps1*, *UAS-TEV*, *rad21*^{TEV}) indicated below the bars. Seventeen mitotic cells from at least four embryos were analyzed for each genotype. Brackets indicate statistically significant differences (*t* test) with ***$p < 0.001$. (C–F) Schematic summary of progression from metaphase (yellow) into anaphase (orange) in embryos with wild-type (C) or excess levels of Mps1 (D–F). In SAC-competent *mad2*$^{+}$ embryos (D), excess Mps1 results in metaphase extension, followed by an almost normal sister chromatid separation during anaphase, presumably because cohesion fatigue during the SAC-dependent metaphase arrest largely counteracts an inhibition of sister chromatid separation by excess Mps1. Without the extended metaphase delay, as in the SAC-deficient *mad2* mutant embryos (E), an essentially complete block of sister chromatid segregation occurs during anaphase, presumably because the SAC-independent inhibition of sister chromatid separation by excess Mps1 is no longer counteracted by cohesion fatigue. However, as predicted by our interpretation, TEV-mediated elimination of cohesion restores an essentially normal sister chromatid segregation in *mad2*-mutant embryos with excess Mps1 (F).

that a more effective removal of sister chromatid cohesion should restore efficient poleward chromatid segregation during anaphase in *mad2*-mutant embryos with excess Mps1 (Figure 7F). To achieve a more effective resolution of sister chromatid cohesion, we performed experiments in embryos that had a cohesin variant with tobacco etch virus (TEV) protease cleavage sites within the Rad21 subunit. This cohesin variant can therefore be opened by TEV protease expression (Pauli *et al.*, 2008). Indeed, TEV protease expression restored chromosome segregation to spindle poles very effectively in *mad2*-mutant embryos with excess Mps1 (Figure 7, A and B). In contrast, in the absence of TEV expression, the *mad2*-mutant embryos with excess Mps1 and TEV-cleavable cohesin displayed the same severe anaphase defects as observed with wild-type cohesin in *mad2*-mutant embryos with excess Mps1 (Figure 7, A and B). These results demonstrate that the failure of chromosome segregation during anaphase resulting from excess Mps1 is caused by inefficient resolution of sister chromatid cohesion and not by insufficient kinetochore attachment. After TEV-mediated cohesion removal, kinetochore attachments are clearly good enough for efficient poleward segregation of sister chromatids in *mad2*-mutant embryos with excess Mps1.

DISCUSSION

Our characterization of *Drosophila* Mps1 revealed a number of novel aspects. Protein kinase activity is not required for Mps1–Mps1 interactions according to our findings with Mps1^{kd}. However, kinase activity seems to be required for Mps1 kinetochore localization in *Drosophila*. Moreover, accurate control of its level and localization is essential for successful mitosis. Both mistargeting and modest overexpression prevent successful mitosis. It is striking that, in addition to inappropriate maintenance of SAC activity, excess Mps1 stabilizes sister chromatid cohesion also in a SAC-independent manner.

In the case of human Mps1, Hewitt *et al.* (2010) demonstrated coimmunoprecipitation of GFP-Mps1 with myc-Mps1. Moreover, coimmunoprecipitation was also observed when both variants carried the D664A mutation, which eliminates kinase activity. Given that these kinase-dead variants were expressed in cells with endogenous wild-type Mps1, it is not entirely excluded that endogenous Mps1 activity might have provided an indispensable contribution for the observed coimmunoprecipitation of the kinase-dead combination. In our experiments, the kinase-dead combination was expressed in larvae, where the great majority of cells are postmitotic and no longer expresses Mps1. Nevertheless, it can still be argued that also in these experiments coimmunoprecipitation would not have occurred in the absence of the minute amounts of residual wild-type Mps1. It is of interest, however, that the kinase-dead combination coimmunoprecipitated in human cells no longer displayed the electrophoretic mobility shifts observed when at least one of the two coimmunoprecipitated versions had a wild-type kinase domain (Hewitt *et al.*, 2010). The results from human cells and *Drosophila* therefore argue very strongly that the Mps1–Mps1 interaction does not depend on Mps1 kinase activity. In this regard human and *Drosophila* Mps1 appear to be identical.

In other respects, human and *Drosophila* Mps1 display some surprisingly different behaviors. The N-terminal regulatory region of human (Liu *et al.*, 2003; Stucke *et al.*, 2004; Xu *et al.*, 2009) but not of *Drosophila* Mps1 is sufficient for kinetochore localization. According to Xu *et al.* (2009), this localization domain, as well as kinase-dead Mps1, is unable to localize to the kinetochore after endogenous Mps1 depletion in human cells. However, several publications reported an opposite result, that is, a more efficient kinetochore localization of human Mps1^{kd} after depletion of endogenous Mps1 (Tighe *et al.*, 2008; Hewitt *et al.*, 2010; Jelluma *et al.*, 2010). Moreover, *Xenopus* Mps1^{kd} still localizes to the kinetochore after immunodepletion of endogenous Mps1 in egg extracts (Abrieu *et al.*, 2001). In addition, several different pharmacological inhibitors of human Mps1 kinase activity have been shown to induce higher levels of Mps1 accumulation at kinetochores (Hewitt *et al.*, 2010; Jelluma *et al.*, 2010; Maciejowski *et al.*, 2010; Santaguida *et al.*, 2010). Thus the majority of studies in vertebrates report kinetochore localization in the absence of Mps1 kinase activity, in contrast to our observations with *Drosophila* Mps1^{kd}.

Although we analyzed a kinase-dead mutation that is identical to the one used in vertebrates, we cannot exclude that this same mutation has different structural consequences in the context of the *Drosophila* protein. Observations with a human Mps1 variant carrying a peroxisome-targeting signal indicated that kinase activation might be linked to substantial conformational changes (Jelluma *et al.*, 2010). The Mps1 variant with the peroxisome-targeting signal was only localized to the peroxisome when it also contained the kinase-dead mutation or when kinase inhibitor was applied. The conformation of active Mps1 kinase therefore appears to be incompatible with a productive interaction between an engineered C-terminal peroxisome-targeting signal and the peroxisome translocation machinery (Jelluma *et al.*, 2010). It seems likely, therefore, that complex conformational changes with decisive effects on localization and activity are involved in Mps1 regulation. In that context, we point out that *Drosophila* Mps1^{kd} is fully capable of interacting with itself *in-trans*, as well as with Mad1, suggesting that its conformation is unlikely to be completely abnormal. Apart from hypothetical differences in conformational behavior, the discordant results concerning dependence of kinetochore localization on Mps1 kinase activity might perhaps also reflect different assay conditions. Nocodazole and MG132 were applied in all the experiments in which increased kinetochore localization of Mps1^{kd} or pharmacologically inhibited Mps1 was observed but not in those in which kinetochore localization was absent (Figure 1D; Xu *et al.*, 2009).

Another difference between human and *Drosophila* Mps1 concerns the consequences of overexpression. As in yeast (Hardwick *et al.*, 1996), modest overexpression of *Drosophila Mps1* (approximately fivefold) is sufficient for SAC hyperactivation and consequent extension of metaphase by more than 10-fold, whereas comparable overexpression in human cells does not have an effect on mitosis (Stucke *et al.*, 2002; Kang *et al.*, 2007; Jelluma *et al.*, 2010). Excess Mps1 in *Drosophila* appears to hyperactivate the SAC directly rather than indirectly via destabilization of kinetochore attachments (Figures 5 and 6). We point out that persistent kinetochore targeting of human Mps1 via fusion to Mis12 also does not destabilize kinetochore attachments (Jelluma *et al.*, 2010), even though it has been demonstrated that human Mps1 can promote transformation of syntelic into amphitelic attachments (Jelluma *et al.*, 2008b; Hewitt *et al.*, 2010; Santaguida *et al.*, 2010; Sliedrecht *et al.*, 2010), similar to yeast Mps1 (Maure *et al.*, 2007).

Experiments in human cells and fission yeast with Mps1 variants (Mis12–Mps1 and Ndc80–Mph1, respectively) that persist at the kinetochore throughout mitosis (Jelluma *et al.*, 2010; Ito *et al.*, 2012) provided strong arguments that the release of Mps1 from kinetochores that occurs during metaphase of unperturbed mitoses is essential for mitotic checkpoint silencing and the transition from metaphase to anaphase. Our experiments in *Drosophila* with similar Mps1 variants (Cenp-C^{C}-Mps1 and Nuf2-Mps1) that also persist at the kinetochore failed to confirm this notion. Our negative evidence might reflect technical difficulties. The fact that the SAC is readily hyperactivated by wild-type *Mps1* overexpression in *Drosophila*

(but not in human cells) clearly complicated our experiments. The amount and activity of Mps1 that was persistently localized at the kinetochore might have been insufficient. Given that EGFP-Cenp-C^C-Mps1 resulted in a failure of sister chromatid segregation during anaphase, our results agree with the findings concerning human Mis12–Mps1 to the extent that both demonstrate the importance of normal Mps1 subcellular localization dynamics.

Failure of sister chromatid segregation during anaphase was not only caused by EGFP-Cenp-C^C-Mps1 but also by overexpression of wild-type *Mps1* in the absence of Mad2. Because sister chromatid segregation was fully restored when cohesion was experimentally removed by TEV expression, we conclude that excess Mps1 inhibits sister chromatid separation. The final separation of sister chromatids immediately before the onset of anaphase is brought about by separase-mediated cleavage of the Rad21 subunit of the cohesion complex (Uhlmann *et al.*, 2000). However, a large fraction of cohesin is released from chromosomes already during prophase and prometaphase in response to Polo and Aurora B kinase activity (Waizenegger *et al.*, 2000). It remains to be analyzed whether Mps1 interferes with these identified pathways of cohesion removal. Our preliminary analyses failed to detect an unusual behavior of Rad21, separase, and Polo. With regard to the inhibitory effect of Mps1 on sister chromatid separation, it also remains to be shown that it is of physiological relevance and not entirely dependent on overexpression. We consider it very likely that a SAC-independent inhibition of sister chromatid separation by endogenous Mps1 is of physiological relevance, as it could provide additional protection against premature sister chromatid separation and consequential aneuploidy.

In *Drosophila*, SAC activation can proceed with breathtaking speed. The time from the start of mitosis until anaphase onset is <3 min during the syncytial cycles of early embryogenesis. Nevertheless, hypoxia, which can be induced very rapidly and causes a relatively subtle effect on microtubule dynamics, triggers a reliable SAC arrest even when generated after mitosis has already started (Fischer *et al.*, 2004; Pandey *et al.*, 2007). SAC-mediated mitotic arrest induction, therefore, requires <3 min in these conditions. In general, rapid and reliable responses to small signals (like a single unattached kinetochore or the slight reduction of microtubule dynamics) involve amplification steps that in turn create a major challenge for timely reversion (Ciliberto and Shah, 2009). We propose that the functional properties of *Drosophila* Mps1 might reflect an evolutionary tuning of SAC speed and efficiency. As a result, even modest overexpression of *Mps1* is already sufficient for SAC activation in *Drosophila*. In addition, the apparent SAC-independent stabilization of sister chromatid cohesion by *Drosophila* Mps1 is likely to provide extra support in the fight against premature sister chromatid separation and consequent aneuploidy. An improved mechanistic understanding of the SAC might also resolve whether the comparatively rapid SAC adaptation in the presence of persistent spindle damage in *Drosophila* reflects design constraints. Moreover, whether Mps1 contributes also in human cells to the control of sister chromatid cohesion in a SAC-independent manner is yet another interesting question for the future.

MATERIALS AND METHODS

Drosophila genetics

All *Drosophila* strains are described in Supplemental Table S1. Genotypes of animals that were used for the collection of data displayed in the figures are specified in Supplemental Table S2. The null alleles of *Mps1* (Page *et al.*, 2007), *mad1* (Emre *et al.*, 2011), *mad2* (Buffin *et al.*, 2007), and *vtd/rad21* (Pauli *et al.*, 2008) that were used for our analyses have been described before, as have the *bubR1^{KEN}* mutants, which are SAC deficient (Rahmani *et al.*, 2009). A chromosome with *P{neoFRT}82B* and *Mps1^{aldB4}*, which allowed for induction of germline clones (Chou and Perrimon, 1996; Fischer *et al.*, 2004), was kindly provided by William D. Gilliland (DePaul University, Chicago, IL).

For expression of *UAS* transgenes in embryos during interphase 14 and analysis of phenotypic consequences during the subsequent mitosis 14, we crossed males carrying such transgenes with *mat-GAL4* females. These females produce eggs containing maternally derived Gal4, which results in activation of strong expression from paternally contributed *UAS* transgenes at onset of zygotic expression during interphase 14.

Hs-GAL4 was used for heat-induced expression of *UAS* transgenes in larvae. For induction of a synchronous progression through embryonic mitosis 14, we used *w*; stg^{7B}, P{w$^+$, Hs-stg}/TM3* as described (Sauer *et al.*, 1995).

For marking chromosomes, centromeres, and spindles for some of the cytological analyses, we used the transgenes *Jupiter-GFP* (Morin *et al.*, 2001), *His2Av-mRFP* and *Cid-EGFP* (Schuh *et al.*, 2007), *mRFP-Cenp-C* (Schittenhelm *et al.*, 2007), and *Tom-Cenp-C* (this study).

For expression of SAC proteins fused to fluorescent tags, we used *GFP-bubR1* (Buffin *et al.*, 2005), *mad1-GFP, mCherry-mad1* (Emre *et al.*, 2011), and *gEGFP-Mps1* (Fischer *et al.*, 2004). The *cis*-regulatory regions of the corresponding genes control expression of these transgenes.

Additional transgenic lines (*gEGFP-Mps1^{kd}*, *gEGFP-Mps1^N*, *gEGFP-Mps1^C*, *UAS-Mps1*, *UAS-EGFP-Mps1*, *UAS-EGFP-Mps1^{kd}*, *UAS-10myc-Mps1*, *UAS-10myc-Mps1^{kd}*, *UAS-EGFP-Cenp-C^C-Mps1*, *UAS-EGFP-Cenp-C^C-Mps1^{kd}*, *UAS-EGFP-Mps1^N*, *UAS-EGFP-Mps1^C*, *UAS-EGFP-Mps1^{Ckd}*, *UAS-EGFP-Mps1-Nuf2*, *UAS-EGFP-Mps1^{kd}-Nuf2*, *UAS-Torso(EC/TM)-EGFP-Mps1*, *UAS-Torso(EC/TM)^{4021}-EGFP-Mps1*, *UAS-EGFP-bub1*, *UAS-EGFP-bubR1*, *UAS-EGFP-bubR1^{kd}*, *UAS-EGFP-Cenp-C^C-bubR1*, *UAS-EGFP-mad2*) were obtained after P element–mediated germline transformation with the constructs described in the Supplemental Material. pUAST constructs were generated for Gal4-mediated expression (Brand and Perrimon, 1993). pCaSpeR4 (Thummel and Pirrotta, 1992) was used for transgene constructs under control of the corresponding normal *cis*-regulatory region. *Mps1^{kd}* codes for the D478A mutation. This mutation abolishes kinase activity (Lince-Faria *et al.*, 2009). *Mps1^N* and *Mps1^C* code for amino acids 1–332 (N-terminal regulatory region) and 325–630 (C-terminal kinase domain), respectively. The C-terminal domain of Cenp-C (Cenp-C^C), which was used to enforce constitutive kinetochore localization of SAC proteins, comprises the amino acids 1009–1411 of the Cenp-C protein. This domain is sufficient for kinetochore localization (Heeger *et al.*, 2005).

For the experiments involving experimental elimination of sister chromatid cohesion before mitosis 14 by TEV expression in *mad2* mutants with excess Mps1, we collected embryos (+TEV, +Rad21^{TEV}, +Mps1 OE) from a cross of *2xrad21^{TEV}/mat-GAL4, His2Av-mRFP, Cid-EGFP; rad21^{ex3}, mad2^P* females with *UAS-TEV, UAS-Mps1 II.4; rad21^{ex3}, mad2^P/TM6* males. For the collection of control embryos without TEV expression (–TEV, +Rad21^{TEV}, +Mps1 OE), the same females were crossed with *UAS-Mps1 II.4; rad21^{ex3}, mad2^P/TM6* males. Additional control embryos (+TEV, –Rad21^{TEV}, +Mps1 OE) were collected from a cross of *mat-GAL4, His2Av-mRFP, Cid-EGFP/+; rad21^{ex3}, mad2^P* females with *UAS-TEV, UAS-Mps1 II.4; rad21^{ex3}; mad2^P/TM6* males. Finally, a cross of *mat-GAL4, His2Av-mRFP, Cid-EGFP/CyO; mad2^P* females with *mad2^P* males was used for the collection of yet other control embryos (–TEV, –Rad21^{TEV}, –Mps1 OE). After in vivo imaging, embryos were genotyped

individually by PCR to distinguish embryos homozygous for *rad21*^{ex3} and *mad2*^{P} from embryos carrying the balancer chromosome *TM6*. Before genotyping, embryos were removed manually from the glass slides, and genomic DNA was prepared using 133 µg/ml proteinase K (Fermentas, Glen Burnie, MD) for 30 min at 50°C in 6 µl of GC reaction buffer for Phusion polymerase (Fermentas) supplied with 0.17% Nonidet P40 Substitute and 0.17% Tween-20. The resulting suspension was used as PCR template. The genetic system for experimental elimination of sister chromatid cohesion before mitosis 14 by TEV expression and its application in *mad2*$^{+}$ embryos has been described (Pauli *et al.*, 2008).

Meiotic recombination was used for the construction of chromosomes with multiple mutations or transgenes. Particular chromosomes were combined by standard crossing schemes to arrive at the stocks used in the experiments (see the Supplemental Material). Because all transgenes were established in a *white* mutant background, we used *w*^{1} flies as wild-type control stock unless otherwise specified.

Microscopy

Embryos were collected on apple juice agar plates and aged to the desired stage. In vivo imaging, fixation, and immunolabeling of *Drosophila* embryos were done essentially as described (Pandey *et al.*, 2005). For in vivo imaging, embryos were dechorionated, immobilized on glass slides, and covered with halocarbon oil. Before fixation, embryos were first dechorionated for 2 min in 7% NaOCl. Embryos were fixed during 1 min with a 1:1 mixture of heptane and methanol. A modified fixation procedure was applied in case of anti-tubulin labeling (Figure 4), which involved preincubation of the dechorionated embryos in 0.73 µM Taxol (Sigma-Aldrich, St. Louis, MO) during 2 min in a 2:1 mixture of heptane and 100 mM 1,4-piperazinediethanesulfonic acid, pH 6.8, 10 mM EDTA, and 20 mM $MgSO_4$ (PEM) before fixation. Subsequently embryos were fixed during 20 min in a 1:1 mixture of heptane and 4% formaldehyde in PEM. The vitelline membrane was removed by shaking for 1 min in a 1:1 mixture of heptane and 90% methanol/50 mM ethylene glycol tetraacetic acid. For immunofluorescence staining, we used rabbit anti-BubR1 (kindly provided by C. Sunkel, Universidade do Porto, Porto, Portugal) at 1:2000 and mouse monoclonal antibody DM1A anti–α-tubulin (Sigma-Aldrich) at 1:8000. DNA was stained with Hoechst 33258 at 1 µg/ml in phosphate-buffered saline. Embryos were mounted in 70% glycerol, 50 mM Tris-HCl, pH 8.5, 5 mM *p*-phenylenediamine, and 50 mM *n*-propylgallate.

Images were acquired with a Zeiss CellObserver HS system (Carl Zeiss, Jena, Germany). For in vivo imaging, we used a 470-nm (GFP) and a 555-nm (mRFP/Tomato) light-emitting diode (LED) as fast-switchable light sources. The 555-nm LED was used in combination with a 550/32 bandpass filter (BrightLine HC; Semrock, Rochester, NY). Emitted signals were detected with a dual bandpass filter (Zeiss 56HE without excitation filter). A 63×/1.4 oil immersion objective was used. Number and spacing of focal planes per time point, as well as time intervals and total duration of the in vivo imaging, were adjusted according to experimental needs.

Single images and movies were processed and evaluated using AxioVision (Zeiss) for region of interest selection, Huygens Remote Manager, version 1.2.3 (Ponti *et al.*, 2007), for deconvolution, Imaris (Bitplane Scientific Software, Zurich, Switzerland) and ImageJ (National Institutes of Health, Bethesda, MD) for measurement of metaphase plate width, sister kinetochore separation, kinetochore velocity, dynamics of progression through mitosis, and kinetochore signal intensities, and Photoshop (Adobe, San Jose, CA) for still-frame processing. Fluorescence intensities of kinetochore signals were measured by integrating pixel intensities within a square encompassing all of the kinetochore signals of a given cell, followed by subtraction of local background values as described previously (Hoffman *et al.*, 2001; Schittenhelm *et al.*, 2010). For width of a metaphase plate, we measured the shortest distance between two parallel lines that were perpendicular to the mitotic spindle and had all of the kinetochore signals in between. The intersister kinetochore distance during early mitosis and the kinetochore segregation distance during exit from mitosis were measured using the distance measurement tool in the Imaris software. The kinetochore segregation velocity was measured by subtracting the interkinetochore distance determined 50 s after anaphase onset from the interkinetochore distance determined at anaphase onset, followed by division of the resulting distance by 50 s.

Extract preparations and immunoprecipitation

Extracts from *Drosophila* embryos for immunoprecipitation were prepared as described (Jäger *et al.*, 2001). Extracts from larvae were prepared analogously using one larva as the equivalent of 50 embryos. For induction of *Hs-GAL4*–mediated *UAS* transgene expression before extract preparation, bottles with larvae were incubated for 2 h in a 37°C water bath, followed by 1 h of recovery at 25°C. Protein extracts from transiently transfected S2R^{+} cells were prepared as described (Furrer *et al.*, 2010). For transient transfection, 300,000 cells were seeded in a T25 flask and cotransfected 24 h later with a combination of *pCaSpeR4-Actin5c-GAL4* and appropriate *pUAST* plasmids using FuGENE HD transfection reagent (Roche, Indianapolis, IN). Extracts were prepared 2 d after transfection. All buffers used for extract preparation were supplemented with protease inhibitor cocktail (P8340; Sigma-Aldrich). For phosphatase treatment, 50 µl of protein extract was incubated for 30 min at 30°C with 1600 U of λ-phosphatase (NEB). We used 50 mM NaF and 10 mM Na_3VO_4 (activated as described; Gordon, 1991) as phosphatase inhibitors. Immunoprecipitation was performed using GFP-Trap coupled to agarose beads (ChromoTek, Martinsried, Germany) or mouse monoclonal antibody 9E10 anti–c-myc (Evan *et al.*, 1985) in combination with protein A–Sepharose beads.

Immunoblotting

Total extracts from *Drosophila* embryos for direct analysis by immunoblotting were prepared by homogenizing the embryos in SDS–PAGE sample buffer. For the preparation of extracts from embryos at defined mitotic stages, we collected eggs from *w*; stg*^{7B}*, P{w*$^{+}$*, Hs-stg}/TM3* flies for 1 h, followed by aging at 25°C for 3 h. *Hs-stg* expression was induced by 15 min of incubation at 37°C. Aliquots of embryos were fixed with methanol either immediately or after recovery at 25°C for 10 and 20 min, respectively. Alternatively, syncytial embryos were collected for 1 h and aged for an additional hour at 25°C, followed by fixation in methanol. After DNA staining with Hoechst 33258, embryos were suspended in a 1:1 mixture of glycerol and EB buffer (Edgar *et al.*, 1994). Embryos in distinct mitotic stages were identified using an inverted fluorescence microscope and pooled before solubilization in SDS–PAGE sample buffer. Discontinuous PAGE was performed according to standard protocols. To increase electrophoretic mobility shifts caused by phosphorylations, Phostag (Wako Chemicals USA, Richmond, VA) was added.

Immunoblots were probed with affinity-purified rabbit antibodies against Mps1 (Rb1) (Pandey *et al.*, 2007) diluted 1:5000, against Mad2 (IS793; a kind gift from D. Sharp, Albert Einstein College of Medicine, New York, NY) diluted 1:1500, against GFP (IS28; Schittenhelm *et al.*, 2007) diluted 1:3000, against GFP (Torrey Pines Biolabs, Secaucus, NJ) diluted 1:5000, and against mRFP (IS743)

diluted 1:3000. These antibodies against mRFP also react with mCherry and are therefore designated as anti-mCherry in the *Results* section. Moreover, we also used mouse monoclonal antibody 9E10 against c-myc diluted 1:15, DM1A against α-tubulin (Sigma-Aldrich) diluted 1:50,000, F2 against cyclin B (Knoblich and Lehner, 1993) diluted 1:3, and ADL67.10 (Stuurman *et al*., 1996) against lamin diluted 1:200. ADL67.10 was obtained from the Developmental Studies Hybridoma Bank (Department of Biology, University of Iowa, Iowa City, IA). Signals were detected by the ECL system (Amersham, Piscataway, NJ). For quantification of proteins by immunoblotting, a dilution series of a reference extract was loaded onto the same gel as the test samples. Nonsaturated exposures, in which the signals obtained for the dilution series were linearly correlated with the loaded amounts, were used for the quantification of the signals in test samples with intensities within the range of those of the dilution series. ImageJ was used for the determination of background-corrected signal intensities.

ACKNOWLEDGMENTS

We are grateful to D. Beuchle, B. Jaunich, S. Moser, C. Sollmann, D. Sharp, C. Sunkel, and W. Gilliland for technical support, antibodies, and fly strains. This study was supported by Swiss National Science Foundation Grant 310003A-120276 (C.F.L.) and the French Agence Nationale de la Recherche (ANR-08-BLAN-0006-01; R.E.K).

REFERENCES

Abrieu A, Magnaghi-Jaulin L, Kahana JA, Peter M, Castro A, Vigneron S, Lorca T, Cleveland DW, Labbe JC (2001). Mps1 is a kinetochore-associated kinase essential for the vertebrate mitotic checkpoint. Cell 106, 83–93.

Basu J, Bousbaa H, Logarinho E, Li Z, Williams BC, Lopes C, Sunkel CE, Goldberg ML (1999). Mutations in the essential spindle checkpoint gene bub1 cause chromosome missegregation and fail to block apoptosis in *Drosophila*. J Cell Biol 146, 13–28.

Brand AH, Perrimon N (1993). Targeted gene expression as a means of altering cell fates and generating dominant phenotypes. Development 118, 401–415.

Buffin E, Emre D, Karess RE (2007). Flies without a spindle checkpoint. Nat Cell Biol 9, 565–572.

Buffin E, Lefebvre C, Huang J, Gagou ME, Karess RE (2005). Recruitment of Mad2 to the kinetochore requires the Rod/Zw10 complex. Curr Biol 15, 856–861.

Cheeseman IM, Chappie JS, Wilson-Kubalek EM, Desai A (2006). The conserved KMN network constitutes the core microtubule-binding site of the kinetochore. Cell 127, 983–997.

Chen RH, Brady DM, Smith D, Murray AW, Hardwick KG (1999). The spindle checkpoint of budding yeast depends on a tight complex between the Mad1 and Mad2 proteins. Mol Biol Cell 10, 2607–2618.

Chou TB, Perrimon N (1996). The autosomal FLP-DFS technique for generating germline mosaics in *Drosophila* melanogaster. Genetics 144, 1673–1679.

Ciferri C *et al*. (2008). Implications for kinetochore-microtubule attachment from the structure of an engineered Ndc80 complex. Cell 133, 427–439.

Ciliberto A, Shah JV (2009). A quantitative systems view of the spindle assembly checkpoint. EMBO J 28, 2162–2173.

Colombo *et al*. (2010). Targeting the mitotic checkpoint for cancer therapy with NMS-P715, an inhibitor of MPS1 kinase. Cancer Res 70, 10255–10264.

Cui Y, Cheng X, Zhang C, Zhang Y, Li S, Wang C, Guadagno TM (2010). Degradation of the human mitotic checkpoint kinase Mps1 is cell cycle-regulated by APC-cCdc20 and APC-cCdh1 ubiquitin ligases. J Biol Chem 285, 32988–32998.

Daum JR, Potapova TA, Sivakumar S, Daniel JJ, Flynn JN, Rankin S, Gorbsky GJ (2011). Cohesion fatigue induces chromatid separation in cells delayed at metaphase. Curr Biol 21, 1018–1024.

DeAntoni A, Sala V, Musacchio A (2005). Explaining the oligomerization properties of the spindle assembly checkpoint protein Mad2. Philos Trans R Soc Lond B Biol Sci 360, 637–647.

DeLuca JG, Dong Y, Hergert P, Strauss J, Hickey JM, Salmon ED, McEwen BF (2005). Hec1 and nuf2 are core components of the kinetochore outer plate essential for organizing microtubule attachment sites. Mol Biol Cell 16, 519–531.

DeLuca JG, Gall WE, Ciferri C, Cimini D, Musacchio A, Salmon ED (2006). Kinetochore microtubule dynamics and attachment stability are regulated by hec1. Cell 127, 969–982.

Dou Z, Sawagechi A, Zhang J, Luo H, Brako L, Yao XB (2003). Dynamic distribution of TTK in HeLa cells: insights from an ultrastructural study. Cell Res 13, 443–449.

Dou Z, von Schubert C, Korner R, Santamaria A, Elowe S, Nigg EA (2011). Quantitative mass spectrometry analysis reveals similar substrate consensus motif for human Mps1 kinase and Plk1. PLoS One 6, e18793.

Edgar BA, Sprenger F, Duronio RJ, Leopold P, O'Farrell PH (1994). Distinct molecular mechanisms regulate cell cycle timing at successive stages of *Drosophila* embryogenesis. Genes Dev 8, 440–452.

Emre D, Terracol R, Poncet A, Rahmani Z, Karess RE (2011). A mitotic role for Mad1 beyond the spindle checkpoint. J Cell Sci 124, 1664–1671.

Espeut J, Gaussen A, Bieling P, Morin V, Prieto S, Fesquet D, Surrey T, Abrieu A (2008). Phosphorylation relieves autoinhibition of the kinetochore motor Cenp-E. Mol Cell 29, 637–643.

Evan GI, Lewis GK, Ramsay G, Bishop JM (1985). Isolation of monoclonal antibodies specific for human c-myc proto-oncogene product. Mol Cell Biol 5, 3610–3616.

Fava LL, Kaulich M, Nigg EA, Santamaria A (2011). Probing the in vivo function of Mad1:C-Mad2 in the spindle assembly checkpoint. EMBO J 30, 3322–3336.

Fischer MG, Heeger S, Hacker U, Lehner CF (2004). The mitotic arrest in response to hypoxia and of polar bodies during early embryogenesis requires *Drosophila* Mps1. Curr Biol 14, 2019–2024.

Fisk HA, Winey M (2001). The mouse Mps1p-like kinase regulates centrosome duplication. Cell 106, 95–104.

Foe VE (1989). Mitotic domains reveal early commitment of cells in *Drosophila* embryos. Development 107, 1–22.

Furrer M, Balbi M, Albarca-Aguilera M, Gallant M, Herr W, Gallant P (2010). *Drosophila* Myc interacts with host cell factor (dHCF) to activate transcription and control growth. J Biol Chem 285, 39623–39636.

Gilliland WD, Hughes SE, Cotitta JL, Takeo S, Xiang Y, Hawley RS (2007). The multiple roles of Mps1 in *Drosophila* female meiosis. PLoS Genet 3, e113.

Gilliland WD, Wayson SM, Hawley RS (2005). The meiotic defects of mutants in the *Drosophila* mps1 gene reveal a critical role of Mps1 in the segregation of achiasmate homologs. Curr Biol 15, 672–677.

Gordon JA (1991). Use of vanadate as protein-phosphotyrosine phosphatase inhibitor. Methods Enzymol 201, 477–482.

Grimison B, Liu J, Lewellyn AL, Maller JL (2006). Metaphase arrest by cyclin E-Cdk2 requires the spindle-checkpoint kinase Mps1. Curr Biol 16, 1968–1973.

Hached K, Xie SZ, Buffin E, Cladiere D, Rachez C, Sacras M, Sorger PK, Wassmann K (2011). Mps1 at kinetochores is essential for female mouse meiosis I. Development 138, 2261–2271.

Hardwick KG, Weiss E, Luca FC, Winey M, Murray AW (1996). Activation of the budding yeast spindle assembly checkpoint without mitotic spindle disruption. Science 273, 953–956.

Heeger S, Leismann O, Schittenhelm R, Schraidt O, Heidmann S, Lehner CF (2005). Genetic interactions of separase regulatory subunits reveal the diverged *Drosophila* Cenp-C homolog. Genes Dev 19, 2041–2053.

Hewitt L, Tighe A, Santaguida S, White AM, Jones CD, Musacchio A, Green S, Taylor SS (2010). Sustained Mps1 activity is required in mitosis to recruit O-Mad2 to the Mad1-C-Mad2 core complex. J Cell Biol 190, 25–34.

Hoffman DB, Pearson CG, Yen TJ, Howell BJ, Salmon ED (2001). Microtubule-dependent changes in assembly of microtubule motor proteins and mitotic spindle checkpoint proteins at PtK1 kinetochores. Mol Biol Cell 12, 1995–2009.

Howell BJ, McEwen BF, Canman JC, Hoffman DB, Farrar EM, Rieder CL, Salmon ED (2001). Cytoplasmic dynein/dynactin drives kinetochore protein transport to the spindle poles and has a role in mitotic spindle checkpoint inactivation. J Cell Biol 155, 1159–1172.

Howell BJ, Moree B, Farrar EM, Stewart S, Fang G, Salmon ED (2004). Spindle checkpoint protein dynamics at kinetochores in living cells. Curr Biol 14, 953–964.

Huang H, Hittle J, Zappacosta F, Annan RS, Hershko A, Yen TJ (2008). Phosphorylation sites in BubR1 that regulate kinetochore attachment, tension, and mitotic exit. J Cell Biol 183, 667–680.

Ito D, Saito Y, Matsumoto T (2012). Centromere-tethered Mps1 pombe homolog (Mph1) kinase is a sufficient marker for recruitment of the

spindle checkpoint protein Bub1, but not Mad1. Proc Natl Acad Sci USA 109, 209–214.
Jäger H, Herzig A, Lehner CF, Heidmann S (2001). *Drosophila* separase is required for sister chromatid separation and binds to PIM and THR. Genes Dev 15, 2572–2584.
Jelluma N, Brenkman AB, McLeod I, Yates JR 3rd, Cleveland DW, Medema RH, Kops GJ (2008a). Chromosomal instability by inefficient Mps1 autoactivation due to a weakened mitotic checkpoint and lagging chromosomes. PLoS One 3, e2415.
Jelluma N, Brenkman AB, van den Broek NJ, Cruijsen CW, van Osch MH, Lens SM, Medema RH, Kops GJ (2008b). Mps1 phosphorylates borealin to control Aurora B activity and chromosome alignment. Cell 132, 233–246.
Jelluma N, Dansen TB, Sliedrecht T, Kwiatkowski NP, Kops GJ (2010). Release of Mps1 from kinetochores is crucial for timely anaphase onset. J Cell Biol 191, 281–290.
Jones MH, Huneycutt BJ, Pearson CG, Zhang C, Morgan G, Shokat K, Bloom K, Winey M (2005). Chemical genetics reveals a role for Mps1 kinase in kinetochore attachment during mitosis. Curr Biol 15, 160–165.
Kang J, Chen Y, Zhao Y, Yu H (2007). Autophosphorylation-dependent activation of human Mps1 is required for the spindle checkpoint. Proc Natl Acad Sci USA 104, 20232–20237.
Kemmler S, Stach M, Knapp M, Ortiz J, Pfannstiel J, Ruppert T, Lechner J (2009). Mimicking Ndc80 phosphorylation triggers spindle assembly checkpoint signalling. EMBO J 28, 1099–1110.
Kinoshita E, Kinoshita-Kikuta E, Koike T (2009). Separation and detection of large phosphoproteins using Phos-tag SDS–PAGE. Nat Protoc 4, 1513–1521.
Knoblich JA, Lehner CF (1993). Synergistic action of *Drosophila* cyclin A and cyclin B during the G2-M transition. EMBO J 12, 65–74.
Kwiatkowski N *et al*. (2010). Small-molecule kinase inhibitors provide insight into Mps1 cell cycle function. Nat Chem Biol 6, 359–368.
Lee S, Thebault P, Freschi L, Beaufils S, Blundell TL, Landry CR, Bolanos-Garcia VM, Elowe S (2012). Characterization of spindle checkpoint kinase Mps1 reveals domain with functional and structural similarities to tetratricopeptide repeat motifs of Bub1 and BubR1 checkpoint kinases. J Biol Chem 287, 5988–6001.
Lince-Faria M, Maffini S, Orr B, Ding Y, Claudia F, Sunkel CE, Tavares A, Johansen J, Johansen KM, Maiato H (2009). Spatiotemporal control of mitosis by the conserved spindle matrix protein megator. J Cell Biol 184, 647–657.
Liu D, Vader G, Vromans MJ, Lampson MA, Lens SM (2009). Sensing chromosome bi-orientation by spatial separation of aurora B kinase from kinetochore substrates. Science 323, 1350–1353.
Liu ST, Chan GK, Hittle JC, Fujii G, Lees E, Yen TJ (2003). Human MPS1 kinase is required for mitotic arrest induced by the loss of CENP-E from kinetochores. Mol Biol Cell 14, 1638–1651.
Logarinho E, Bousbaa H, Dias JM, Lopes C, Amorim I, Antunes-Martins A, Sunkel CE (2004). Different spindle checkpoint proteins monitor microtubule attachment and tension at kinetochores in *Drosophila* cells. J Cell Sci 117, 1757–1771.
Luo X, Tang Z, Rizo J, Yu H (2002). The Mad2 spindle checkpoint protein undergoes similar major conformational changes upon binding to either Mad1 or Cdc20. Mol Cell 9, 59–71.
Maciejowski J, George KA, Terret ME, Zhang C, Shokat KM, Jallepalli PV (2010). Mps1 directs the assembly of Cdc20 inhibitory complexes during interphase and mitosis to control M phase timing and spindle checkpoint signaling. J Cell Biol 190, 89–100.
Maldonado M, Kapoor TM (2011). Constitutive Mad1 targeting to kinetochores uncouples checkpoint signalling from chromosome biorientation. Nat Cell Biol 13, 475–482.
Mapelli M, Massimiliano L, Santaguida S, Musacchio A (2007). The Mad2 conformational dimer: structure and implications for the spindle assembly checkpoint. Cell 131, 730–743.
Martin-Lluesma S, Stucke VM, Nigg EA (2002). Role of Hec1 in spindle checkpoint signaling and kinetochore recruitment of Mad1/Mad2. Science 297, 2267–2270.
Mattison CP, Old WM, Steiner E, Huneycutt BJ, Resing KA, Ahn NG, Winey M (2007). Mps1 activation loop autophosphorylation enhances kinase activity. J Biol Chem 282, 30553–30561.
Maure JF, Kitamura E, Tanaka TU (2007). Mps1 kinase promotes sister-kinetochore bi-orientation by a tension-dependent mechanism. Curr Biol 17, 2175–2182.
Morin X, Daneman R, Zavortink M, Chia W (2001). A protein trap strategy to detect GFP-tagged proteins expressed from their endogenous loci in *Drosophila*. Proc Natl Acad Sci USA 98, 15050–15055.
Musacchio A, Salmon ED (2007). The spindle-assembly checkpoint in space and time. Nat Rev Mol Cell Biol 8, 379–393.
O'Tousa J (1982). Meiotic chromosome behavior influenced by mutation-altered disjunction in *Drosophila* melanogaster females. Genetics 102, 503–524.
Oliveira RA, Coelho PA, Sunkel CE (2005). The condensin I subunit Barren/CAP-H is essential for the structural integrity of centromeric heterochromatin during mitosis. Mol Cell Biol 25, 8971–8984.
Page SL, Nielsen RJ, Teeter K, Lake CM, Ong S, Wright KR, Dean KL, Agne D, Gilliland WD, Hawley RS (2007). A germline clone screen for meiotic mutants in *Drosophila* melanogaster. Fly (Austin) 1, 172–181.
Palframan WJ, Meehl JB, Jaspersen SL, Winey M, Murray AW (2006). Anaphase inactivation of the spindle checkpoint. Science 313, 680–684.
Pandey R, Heeger S, Lehner CF (2007). Rapid effects of acute anoxia on spindle kinetochore interactions activate the mitotic spindle checkpoint. J Cell Sci 120, 2807–2818.
Pandey R, Heidmann S, Lehner CF (2005). Epithelial re-organization and dynamics of progression through mitosis in *Drosophila* separase complex mutants. J Cell Sci 118, 733–742.
Pauli A, Althoff F, Oliveira RA, Heidmann S, Schuldiner O, Lehner CF, Dickson BJ, Nasmyth K (2008). Cell-type-specific TEV protease cleavage reveals cohesin functions in *Drosophila* neurons. Dev Cell 14, 239–251.
Ponti A, Gulati A, Bäcker V, Schwarb P (2007). Huygens remote manager: a web interface tool for high-volume batch deconvolution. Imag Microsc 9, 57–58.
Rahmani Z, Gagou ME, Lefebvre C, Emre D, Karess RE (2009). Separating the spindle, checkpoint, and timer functions of BubR1. J Cell Biol 187, 597–605.
Santaguida S, Tighe A, D'Alise AM, Taylor SS, Musacchio A (2010). Dissecting the role of MPS1 in chromosome biorientation and the spindle checkpoint through the small molecule inhibitor reversine. J Cell Biol 190, 73–87.
Sauer K, Knoblich JA, Richardson H, Lehner CF (1995). Distinct modes of cyclin E/cdc2c kinase regulation and S phase control in mitotic and endoreduplication cycles of *Drosophila* embryogenesis. Genes Dev 9, 1327–1339.
Saurin AT, van der Waal MS, Medema RH, Lens SM, Kops GJ (2011). Aurora B potentiates Mps1 activation to ensure rapid checkpoint establishment at the onset of mitosis. Nat Commun 2, 316.
Schittenhelm RB, Althoff F, Heidmann S, Lehner CF (2010). Detrimental incorporation of excess Cenp-A/Cid and Cenp-C into *Drosophila* centromeres is prevented by limiting amounts of the bridging factor Cal1. J Cell Sci 123, 3768–3779.
Schittenhelm RB, Heeger S, Althoff F, Walter A, Heidmann S, Mechtler K, Lehner CF (2007). Spatial organization of a ubiquitous eukaryotic kinetochore protein network in *Drosophila* chromosomes. Chromosoma 116, 385–402.
Schuh M, Lehner CF, Heidmann S (2007). Incorporation of *Drosophila* CID/CENP-A and CENP-C into centromeres during early embryonic anaphase. Curr Biol 17, 237–243.
Shimogawa MM *et al*. (2006). Mps1 phosphorylation of Dam1 couples kinetochores to microtubule plus ends at metaphase. Curr Biol 16, 1489–1501.
Sironi L, Mapelli M, Knapp S, De Antoni A, Jeang KT, Musacchio A (2002). Crystal structure of the tetrameric Mad1-Mad2 core complex: implications of a "safety belt" binding mechanism for the spindle checkpoint. EMBO J 21, 2496–2506.
Skoufias DA, Andreassen PR, Lacroix FB, Wilson L, Margolis RL (2001). Mammalian mad2 and bub1/bubR1 recognize distinct spindle-attachment and kinetochore-tension checkpoints. Proc Natl Acad Sci USA 98, 4492–4497.
Sliedrecht T, Zhang C, Shokat KM, Kops GJ (2010). Chemical genetic inhibition of Mps1 in stable human cell lines reveals novel aspects of Mps1 function in mitosis. PLoS One 5, e10251.
Stevens D, Gassmann R, Oegema K, Desai A (2011). Uncoordinated loss of chromatid cohesion is a common outcome of extended metaphase arrest. PLoS One 6, e22969.
Stucke VM, Baumann C, Nigg EA (2004). Kinetochore localization and microtubule interaction of the human spindle checkpoint kinase Mps1. Chromosoma 113, 1–15.
Stucke VM, Sillje HH, Arnaud L, Nigg EA (2002). Human Mps1 kinase is required for the spindle assembly checkpoint but not for centrosome duplication. EMBO J 21, 1723–1732.
Stuurman N, Sasse B, Fisher PA (1996). Intermediate filament protein polymerization: molecular analysis of *Drosophila* nuclear lamin head-to-tail binding. J Struct Biol 117, 1–15.

Sun T, Yang X, Wang W, Zhang X, Xu Q, Zhu S, Kuchta R, Chen G, Liu X (2010). Cellular abundance of Mps1 and the role of its carboxyl terminal tail in substrate recruitment. J Biol Chem 285, 38730–38739.

Taylor SS, Hussein D, Wang Y, Elderkin S, Morrow CJ (2001). Kinetochore localisation and phosphorylation of the mitotic checkpoint components Bub1 and BubR1 are differentially regulated by spindle events in human cells. J Cell Sci 114, 4385–4395.

Thummel CS, Pirrotta V (1992). Technical Notes: new pCaSpeR P-element vectors. *Drosophila* Inf Newsl 71, 150.

Tighe A, Staples O, Taylor S (2008). Mps1 kinase activity restrains anaphase during an unperturbed mitosis and targets Mad2 to kinetochores. J Cell Biol 181, 893–901.

Uhlmann F, Wernic D, Poupart MA, Koonin EV, Nasmyth K (2000). Cleavage of cohesin by the CD clan protease separin triggers anaphase in yeast. Cell 103, 375–386.

Vigneron S, Prieto S, Bernis C, Labbe JC, Castro A, Lorca T (2004). Kinetochore localization of spindle checkpoint proteins: who controls whom? Mol Biol Cell 21, 21.

Waizenegger IC, Hauf S, Meinke A, Peters JM (2000). Two distinct pathways remove mammalian cohesin from chromosome arms in prophase and from centromeres in anaphase. Cell 103, 399–410.

Wang W *et al.* (2009). Structural and mechanistic insights into Mps1 kinase activation. J Cell Mol Med 13, 1679–1694.

Welburn JP, Vleugel M, Liu D, Yates JR 3rd, Lampson MA, Fukagawa T, Cheeseman IM (2010). Aurora B phosphorylates spatially distinct targets to differentially regulate the kinetochore-microtubule interface. Mol Cell 38, 383–392.

Wojcik E, Basto R, Serr M, Scaerou F, Karess R, Hays T (2001). Kinetochore dynein: its dynamics and role in the transport of the Rough deal checkpoint protein. Nat Cell Biol 3, 1001–1007.

Wong OK, Fang G (2006). Loading of the 3F3/2 antigen onto kinetochores is dependent on the ordered assembly of the spindle checkpoint proteins. Mol Biol Cell 17, 4390–4399.

Xu Q, Zhu S, Wang W, Zhang X, Old W, Ahn N, Liu X (2009). Regulation of kinetochore recruitment of two essential mitotic spindle checkpoint proteins by Mps1 phosphorylation. Mol Biol Cell 20, 10–20.

Zhang X, Yin Q, Ling Y, Zhang Y, Ma R, Ma Q, Cao C, Zhong H, Liu X, Xu Q (2011). Two LXXLL motifs in the N terminus of Mps1 are required for Mps1 nuclear import during G(2)/M transition and sustained spindle checkpoint responses. Cell Cycle 10, 2742–2750.

Zhao Y, Chen RH (2006). Mps1 phosphorylation by MAP kinase is required for kinetochore localization of spindle-checkpoint proteins. Curr Biol 16, 1764–1769.

Zich J, Sochaj AM, Syred HM, Milne L, Cook AG, Ohkura H, Rappsilber J, Hardwick KG (2012). Kinase activity of fission yeast mph1 is required for mad2 and mad3 to stably bind the anaphase promoting complex. Curr Biol 22, 296–301.